mice harboring the core gene, increased ROS production has been observed.[7-9] A recent study found, by the proteomic profiling of biopsy specimens, that an impairment in key mitochondrial processes, including fatty acid oxidation and oxidative phosphorylation, and in the response to oxidative stress occurs in HCV-infected human liver with advanced fibrosis.[10] Therefore, it is probable that the HCV core protein affects mitochondrial functions because such pathogenesis is observed in both HCV core-transgenic mice and HCV-infected patients.[11-13]

The recent progress in proteomics has opened new avenues for disease-related biomarker discovery. Among proteomics approaches, two-dimensional polyacrylamide gel electrophoresis (2D-PAGE) is a technique for the separation and identification of proteins in a sample by displacement in two dimensions oriented at right angles to one another. This method is generally used as a component of proteomics and is the step used for the isolation of proteins for further characterization by mass spectrometry. 2D-PAGE is particularly useful when comparing two related samples such as healthy and diseased tissue. For example, proteins that are more abundant in diseased tissue may represent novel drug targets or diagnostic markers. In fact, several candidate biomarkers for many human cancers have been identified by this approach.[14] There are, however, tens of thousands of proteins in a cell, differing in abundance over six orders of magnitude. 2D-PAGE is not sensitive enough to detect rare proteins, and hence many proteins are not resolved. Therefore, splitting a sample into different fractions is often necessary to reduce the complexity of protein mixtures prior to 2D-PAGE. For this advantage, Lescuyer et al.[15] performed a 2D-PAGE of human mitochondrial proteins derived from the placenta and identified proteins mainly by peptide mass fingerprinting.

In this study, we performed a 2D-PAGE of mitochondria isolated from HepG2 cells stably expressing the HCV core protein and identified several proteins of different expressions when compared with control HepG2 cells. Among up-regulated proteins in the core-expressing cells, we focused on prohibitin, which functions as a mitochondrial protein chaperon, and found that the core protein interacts with prohibitin and represses the interaction between prohibitin and subunit proteins of cytochrome c oxidase (COX), which may lead to decreases in the expression level of the proteins and in COX activity. These results may explain the pathogenesis of liver disease in HCV infection including ROS induction.

Materials and Methods

Cells and Purification of Mitochondria. Hep39 cells,[16] which stably express the HCV core protein, and control HepG2 cells (Hepswx) were grown in Dulbecco's modified Eagle medium (DMEM) containing 10% fetal bovine serum and 1 mg/mL G418. Mitochondria were purified using Nycodenz (Nycomed Pharma, Zürich, Switzerland) according to the protocols reported by Okado-Matsumoto et al.[17] For transient transfection experiments, HepG2 cells were transfected with a core-expression plasmid using TransIT-LT1 (Mirus Bio, Madison, WI). Huh7 cells harboring HCV genotype 1b full-genomic (RCYM1)[18] or subgenomic replicon (5-15), and livers of 3-month-old core-gene transgenic mice[2] were also used for the analysis.

2D-PAGE. Gel electrophoresis in the first dimension was performed using an immobilized pH gradient gel (Immobiline Dry Strip gel, pH 4-7 linear, 13 cm; GE Healthcare, Uppsala, Sweden). The two-dimensional separation was performed on 12.5%, 14 × 16 cm^2, SDS polyacrylamide gels. After the electrophoresis, gels were silver-stained using a silver staining kit (GE Healthcare) according to the manufacturer's protocols. The stained gels were scanned and electronic images of the gels were analyzed using ImageMaster 2D Elite software (GE Healthcare).

In-Gel Digestion and Matrix-Assisted Laser Desorption Ionization, Time-of-Flight Mass Spectrometry (MALDI-TOF-MS). Protein spots on the gels were excised and a "control" piece was cut from a blank region of the gel and processed in parallel with the sample. In-gel digestion with trypsin was performed as reported.[19] The resulting peptides were concentrated using Zip-Tip C18 (Millipore, Bedford, MA). The peptide mixtures were eluted from Zip-Tip with 75% acetonitrile in 0.1% trifluoroacetic acid (TFA). The matrix (α-cyano-4-hydroxycinnamic acid dissolved in 50% acetonitrile, 0.1% TFA) was deposited on a dried sample target. Then 0.5-μL aliquots of the analyte solution were deposited onto matrix surfaces and the solvent was allowed to evaporate at ambient temperature. The digests were analyzed with a TOF mass spectrometer, PE Biosystems Voyager DE STR MALDI (Foster City, CA).

Database Analysis. For protein identification the measured monoisotopic masses of the peptides were analyzed using MS-Fit provided by UCSF (http://prospector.ucsf.edu/ucsfhtml3.2/msfit.htm).

Immunoblotting and Immunoprecipitation. Purified mitochondria were lysed and sonicated in RIPA buffer, then centrifuged at 16,000 rpm for 10 minutes. Protein concentration was determined using a BCA Protein Assay Reagent Kit (Pierce Biotechnology, Rockford, IL). The samples were separated by sodium dodecyl sulfate (SDS)-PAGE and electrotransferred onto a polyvinylidene fluoride membrane (Immobilon; Millipore, Japan), then blocked with BlockAce (Snow Brand, To-

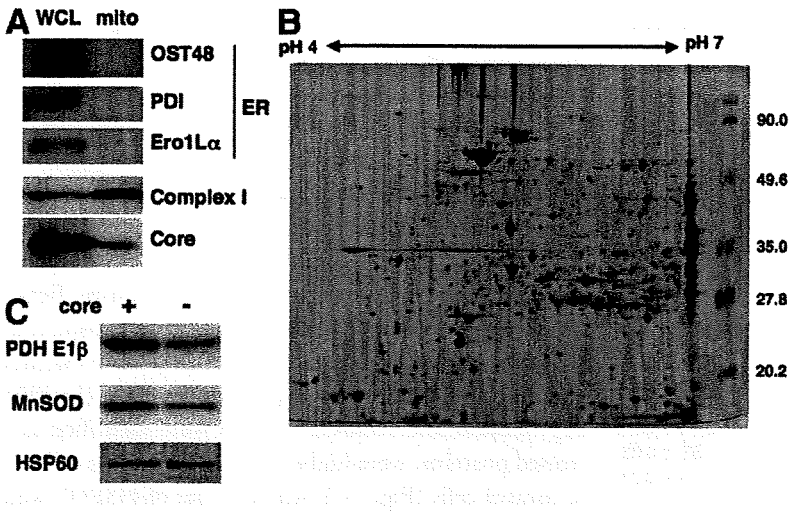

Fig. 1. 2D-PAGE of mitochondria purified from core-expressing cells. (A) Whole-cell lysates (WCL) and purified mitochondria (mito) derived from core-expressing cells were subjected to SDS-PAGE and immunoblotted with anti-core, anti-subunit of complex I (mitochondrial protein), or anti-OST48, PDI, Ero1La (ER proteins) antibodies. (B) Purified mitochondria of core-expressing cells were subjected to 2D-PAGE and the gel was stained with silver. The numbers shown on the right are molecular weights. (C) Purified mitochondria of core-expressing and control cells were subjected to SDS-PAGE and blotted with an anti-E1β subunit of PDH (PDH E1β), anti-MnSOD, or anti-HSP60 antibody.

kyo, Japan). The membrane was subsequently incubated with specific primary antibodies followed by horseradish peroxidase-conjugated secondary antibodies and visualized using SuperSignal West Pico Chemiluminescent Substrate (Pierce). Antibodies against the core protein (Anogen, Mississauga, Canada), manganese superoxide dismutase (MnSOD) (BD Biosciences, San Jose, CA), prohibitin (Neomarkers, Fremont, CA), oligosaccharyltransferase-48 (OST48), heat shock protein (HSP) 60 (Santa-Cruz Biotechnology, Santa Cruz, CA), pyruvate dehydrogenase (PDH), ubiquinol-cytochrome c oxidoreductase, COX (Molecular Probes, Eugene, OR), protein disulfide isomerase (PDI), ER protein endoplasmic oxidoreduction-1 (Ero1)-Lα, and IκBα (Cell Signaling Technology, Danvers, MA), were used as primary antibodies. For immunoprecipitation experiments, cells were lysed in NET-N buffer (20 mM Tris-HCl [pH 8.0], 100 mM NaCl, 1 mM EDTA, 0.5% Nonidet P-40) and the lysates were incubated with anti-prohibitin overnight followed by the addition of protein Sepharose 4B (GE Healthcare), then washed with the same buffer five times. Immunoprecipitates were subjected to SDS-PAGE followed by immunoblotting with specific antibodies.

Determination of COX Activity. COX activity was determined with a MitoProfile Rapid Microplate Assay Kit (MitoSciences, Eugene, OR) using 10 μg of purified mitochondria. The assay was performed three times independently.

Statistical Analysis. Results are expressed as means $\pm$ SE. The significance of the difference in means was determined by Student's t test or Mann-Whitney's U test.

Results

Presence of HCV Core Protein in Purified Mitochondria. Increasing evidence suggests that the HCV core protein is localized to mitochondria as well as to ER and the nucleus. Therefore, we first investigated whether the core protein is expressed in the mitochondria of core-expressing (Hep39) cells used in this study. We used Nycodenz discontinuous gradients to extract mitochondria as described.[17] In the mitochondria derived from core-expressing HepG2 cells, the core protein was detected by immunoblotting, whereas ER resident proteins such as an ER-specific type I transmembrane protein OST48, ER-resident molecular chaperon PDI, and ER membrane-associated N-glycoprotein Ero1-Lα, were not (Fig. 1A). In this fraction, reduced nicotinamide adenine dinucleotide (NADH)-ubiquinone oxidoreductase, complex I of mitochondrial oxidative phosphorylation system, was more strongly expressed than that in the whole cell. These results indicate that the purified mitochondria fraction was free of ER, and that a portion of the core protein was localized to the mitochondria in core-expressing cells.

Proteomics Analysis of Mitochondria by 2D-PAGE. For proteomics analysis, purified mitochondrial proteins derived from core-expressing cells were subjected to 2D-PAGE followed by silver-staining of the gel. In this study we analyzed only acidic proteins using IPG strips covering pH 4 to pH 7 because the analysis of acidic proteins by 2D-PAGE is relatively easy. The mitochondrial fraction was also extracted from Hepswx, a control cell line resistant to G418 but does not express the core protein, then similarly subjected to 2D-PAGE and used for comparing the expression pattern. We repeated the above procedure (purification of mitochondria, 2D-PAGE, and silver-staining) five times, and confirmed a similar expression pattern in core-expressing cells. The representative gel image is shown in Fig. 1B. ImageMaster 2D Elite software detected about 1100 spots on the silver-stained acidic gel, i.e., at pH 4-7 and Mrs of 20-100 kDa. The number of

Table 1. Proteins of Differential Expression in Mitochondria of Core-Expressing Cells

Protein Name	Fold Change (Mean ± SD)
Increased	
Succinyl-CoA:ketoacid CoA transferase	10.43 ± 1.29
NADH-specific isocitrate dehydrogenase a subunit precursor	9.64 ± 4.66
Unknown	8.65 ± 2.40
GrpE-like protein co-chaperon	5.71 ± 0.49
Leucine aminopeptidase	4.26 ± 1.14
Pyruvate dehydrogenase E1 component b subunit	3.79 ± 1.34
CG015alt2	3.18 ± 0.80
HSP70	3.11 ± 1.39
Prohibitin	2.60 ± 0.24
3-Hydroxyisobutyrate dehydrogenase	2.47 ± 0.77
HSPC108	2.46 ± 0.69
MnSOD	2.35 ± 0.65
Ubiquinol-cytochrome c oxidoreductase core I protein	2.00 ± 0.23
Decreased	
Aldehyde dehydrogenase 2	0.12 ± 0.02
Aldehyde dehydrogenase 5 precursor	0.25 ± 0.03
ATP synthase a subunit isoform 1	0.50 ± 0.09
Reference protein	
HSP60	1.02 ± 0.02

protein spots was smaller than those reported in a recent study investigating the human placental mitochondrial proteome.[15]

We then compared the intensity of the spots between core-expressing and control cells. Analysis of repeated experiments by Student's t test revealed 13 increased and three decreased spots in intensity in core-expressing cells. These spots were excised and digested with trypsin, then proteins were identified by mass spectrometry. The names of the identified proteins are listed in Table 1. Among them were proteins related to mitochondrial respiratory chain, protein chaperons, and lipid metabolism. Because antibodies to some of these proteins are commercially available, expression levels of the proteins were examined by immunoblotting. The expression levels of the PDH-E1β subunit and MnSOD, which were identified as increased proteins, were higher in core-expressing cells than in control cells (Fig. 1C), whereas that of HSP60, which was identified as having a similar expression, was unchanged.

Up-regulation of Prohibitin by the Core Protein. Among the identified proteins, we focused on prohibitin, an up-regulated protein in mitochondria of core-expressing cells (Fig. 2A). Prohibitin is a mitochondrial protein associated with cell proliferation.[20] It also works as a chaperon of mitochondrial proteins.[21,22] We confirmed an increased prohibitin expression level in core-expressing cells

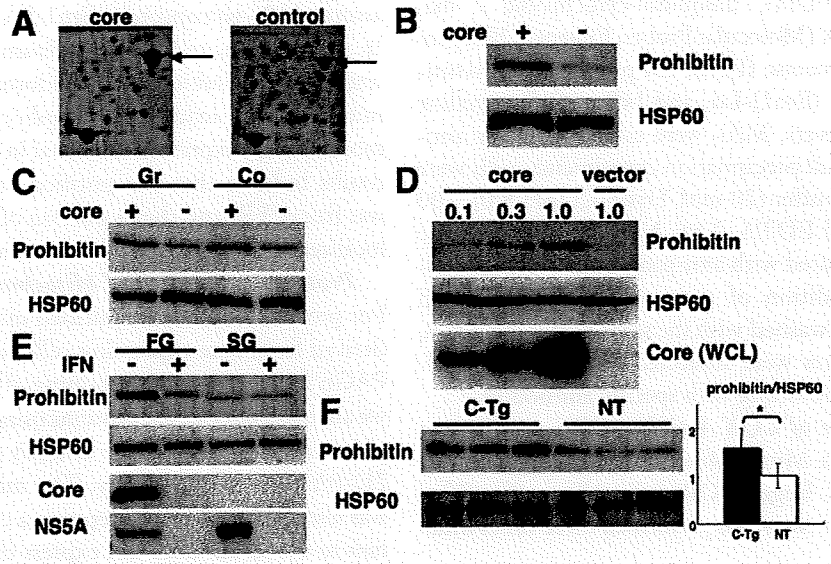

Fig. 2. Up-regulation of prohibitin in core-expressing cells. (A) Protein spot corresponding to prohibitin (arrow) in 2D-PAGE. (B) Purified mitochondria from core-expressing or control cells were subjected to SDS-PAGE and immunoblotted with anti-prohibitin or anti-HSP60 antibody. (C) Mitochondria were purified from growing (Gr) or confluent (Co) cells in 100-mm dishes and subjected to SDS-PAGE, then immunoblotted with an anti-prohibitin or anti-HSP60 antibody. (D) HepG2 cells in six-well plates were transfected with different amounts (μg) of core-expressing plasmid and mitochondrial proteins were analyzed by immunoblotting with anti-prohibitin or anti-HSP60 antibody. The expression levels of the core protein in whole-cell lysates (WCL) were also determined. (E) Cells harboring HCV replicon were untreated or treated with IFN and expression levels of prohibitin in mitochondria were determined. Expression of HCV core and NS5A proteins was also examined. FG, full-genomic replicon cells; SG, subgenomic replicon cells. (F) Expression levels of prohibitin in mitochondria were determined in liver tissues HCV core-gene transgenic and nontransgenic mice. Prohibitin/HSP60 expression levels were determined by densitometry. C-Tg, core-gene transgenic mouse; NT, nontransgenic littermate (n = 3) *$P < 0.05$.

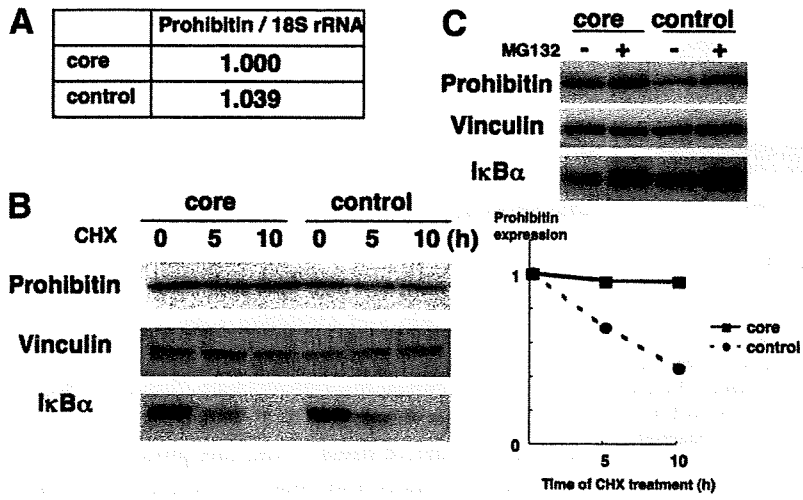

Fig. 3. Increased protein stability of prohibitin in core-expressing cells. (A) RNA was extracted from core-expressing and control cells, and the amount of specific mRNA was determined by real-time PCR with specific primers/probe against prohibitin. The amount of prohibitin mRNA was standardized by that of 18S ribosomal RNA (18S rRNA). (B) Cells were incubated with 100 ng/mL cycloheximide and harvested at the timepoints indicated above the lanes (numbers are hours of cycloheximide treatment). Whole-cell lysates were subjected to SDS-PAGE and immunoblotted with anti-prohibitin, anti-IκBα, or anti-vinculin (as an internal standard) antibody. The intensity of each band was measured by densitometry, and expression levels (prohibitin/vinculin) are shown in the right panel. (C) Cells were harvested after incubation with 20 μM MG132 for 8 hours and subjected to immunoblotting with anti-prohibitin, anti-IκBα, or anti-vinculin antibody.

by immunoblotting (Fig. 2B). Because prohibitin is associated with cell proliferation, it is possible that prohibitin expression changed according to the cell proliferative status. As shown in Fig. 2C, core-expressing cells had high prohibitin expression levels in the cells in both confluent growth and growing statuses compared with control cells. We also determined the expression levels in cells synchronized with aphidicolin followed by l-mimosine treatment and found an increased expression level in core-expressing cells (data not shown). To exclude the possibility that the increased prohibitin expression level is due to the expansion of limited cell clones, not specific to the core protein expression, we examined prohibitin expression in cells transiently expressing the core protein and found that prohibitin expression level increased dose-dependently in core-expressing cells (Fig. 2D). We also examined the prohibitin expression levels in Huh7 cells harboring full- or subgenomic HCV replicon. For this purpose, we used interferon (IFN)-treated replicon cells (cured cells) as a control. Core and nonstructural (NS)5A proteins were not detected after treatment of full-genomic replicon cells with IFN, suggesting a successful elimination of replicon. Prohibitin expression levels in cells with full-genomic replicon were increased compared with those in IFN-treated cured cells, whereas levels of prohibitin expression were low in subgenomic replicon cells regardless of IFN-treatment (Fig. 2E). In addition, prohibitin expression levels were also increased in livers of 3-month-old transgenic mice expressing the core protein compared with those in nontransgenic littermates (Fig. 2F).

We next sought to determine the mechanism of the increased steady-state level of prohibitin in core-expressing cells. To determine prohibitin messenger RNA (mRNA) expression, we performed a real-time polymerase chain reaction (PCR) using specific primers/probe. No difference in prohibitin mRNA was observed between core-expressing and control cells (Fig. 3A). We next determined the stability of prohibitin in these cells. By treating the cells with cycloheximide, the expression levels of prohibitin gradually decreased in control cells (Fig. 3B). On the other hand, in core-expressing cells prohibitin was hardly degraded by cycloheximide treatment for 10 hours, whereas IκBα was equally degraded in both cells. This result suggests that prohibitin was stabilized in the presence of the core protein. Because prohibitin has been shown to be degraded by proteasome,[23] we examined expression levels of prohibitin in the presence of proteasome inhibitor MG132. By treatment with MG132, prohibitin expression was increased to the similar level in core-expressing and control cells. These results suggest that the core protein may inhibit proteasomal degradation of prohibitin by some mechanism, including the prevention of degradation by interaction with the core protein. Then, core-expressing cells were lysed and subjected to immunoprecipitation with an anti-prohibitin antibody. As shown in Fig. 4, the core protein was coimmunoprecipitated with an anti-prohibitin antibody. To exclude a nonspecific interaction with the antibody or Sepharose beads, cells expressing a small amount of prohibitin by transfection with small interfering RNA (siRNA) against prohibitin were also examined. In these cells the amount of the coimmunoprecipitated core protein decreased. In addition, the core protein was not coimmunoprecipitated by control immunoglobulin G (IgG), indicating a specific interaction of prohibitin with the core protein. These results suggest that prohibitin expression increased in core-expressing cells owing to the increased stability presumably by interaction with the core protein.

Impaired Chaperon Function of Prohibitin in Core-Expressing Cells. We next examined the effect of

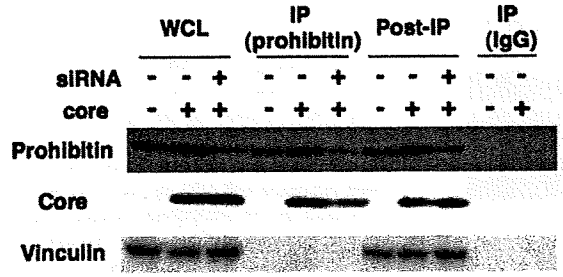

Fig. 4. Interaction of the core protein with prohibitin. Core-expressing and control cells were transfected with or without siRNA against the prohibitin gene, then harvested and lysed in NET-N buffer 3 days after transfection. Whole-cell lysates (WCL) were immunoprecipitated (IP) with an anti-prohibitin antibody or control IgG and immunoblotted with anti-prohibitin or anti-core antibody. Supernatants after the immunoprecipitation were harvested and similarly immunoblotted (Post-IP).

the interaction of prohibitin with the core protein on the function of prohibitin. Prohibitin works as a chaperon of mitochondrial proteins. Nijtmans et al.[21] demonstrated that prohibitin exerts a chaperon function particularly for the stabilization of mitochondrial DNA-encoded proteins. COX is a mitochondrial respiratory complex IV formed by 14 subunits, 10 of which are encoded by nuclear DNA and the rest by mitochondrial DNA.[24] We examined the interaction of prohibitin with subunit II of COX encoded by mitochondrial DNA. As shown in Fig. 5A, the level of COX II coimmunoprecipitated with an anti-prohibitin antibody was decreased in core-expressing cells, although the amount of immunoprecipitated prohibitin was higher than that in control cells. On the other hand, the subunit IV of COX encoded by nuclear DNA was similarly coimmunoprecipitated between core-expressing and control cells. When prohibitin expression was decreased by siRNA transfection, coimmunoprecipitation of COX subunits was similarly decreased with the amount of immunoprecipitation of prohibitin itself being low. We next determined expression levels of COX subunits in the mitochondria in these cells. Expression levels of mitochondrial DNA-encoded subunits I and II in core-expressing cells were decreased, whereas the levels of nuclear DNA-encoded subunits IV and VIb were similar to those in control cells. When transfected with prohibitin-siRNA, expression levels of all of the COX subunits examined were decreased in both core-expressing and control cells, suggesting that protein levels of these subunits are dependent on prohibitin (Fig. 5B, see Supporting Fig. 1 for densitometry). Similar data were observed when blots for COX II and IV were developed together in the same membrane (Supporting Fig. 2). We also determined COX activity in these cells and found that core-expressing cells had a significantly decreased COX activity (about 70% of that in control cells, Fig. 5C). These results suggest that interaction of prohibitin with the core protein is associated with an impaired function of prohibitin as a mitochondrial chaperon, which may trigger disordered assembly and function of mitochondrial respiratory complexes.

Discussion

In the present study we analyzed expression levels of mitochondrial proteins in HepG2 cells expressing the HCV core protein and identified a set of proteins with different expressions. Some of those proteins were related to the mitochondrial respiratory chain (Table 1). Because the core protein was shown to be associated with the induction of oxidative stress,[7-9] the core protein may modulate the expression and function of proteins forming mitochondrial respiratory complexes, which naturally

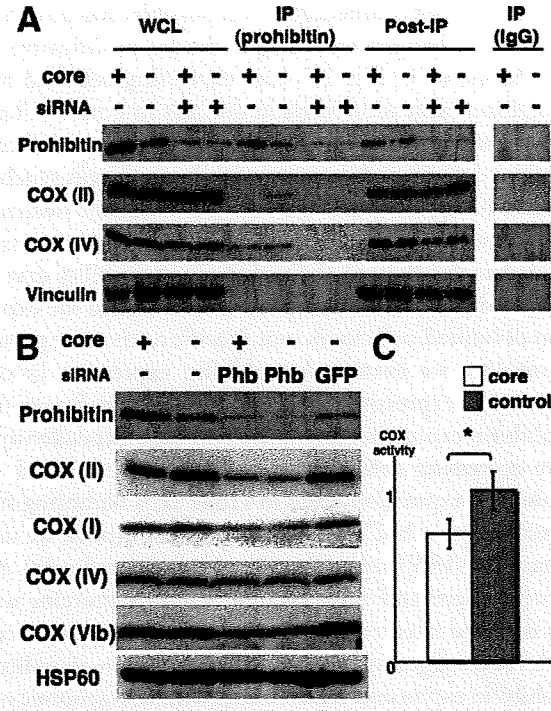

Fig. 5. Effects of core-prohibitin interaction on interaction/expression of COX subunit proteins and COX activity. (A) Whole-cell lysates (WCL) of core-expressing and control cells were subjected to immunoprecipitation with an anti-prohibitin antibody or control IgG, and the interaction of prohibitin with COX subunits was determined by immunoblotting of immunoprecipitated proteins (IP). Supernatants after the immunoprecipitation were harvested and similarly immunoblotted (Post-IP). (B) Cells were transfected with or without siRNA against the prohibitin (Phb) or GFP gene and harvested 3 days after transfection for purification of mitochondria. Purified mitochondria were subjected to SDS-PAGE and immunoblotted with several anti-COX subunits antibodies. The expression levels of HSP60 were also examined as an internal control. (C) COX activity was determined by measuring cytochrome c oxidation. The activity was normalized by taking the average rate of control cells as 1. Data shown are means ± SE ($n = 5$). $^*P < 0.05$.

leads to ROS accumulation. In addition, MnSOD, which plays a key role in protecting cells from oxidative damage, was up-regulated in core-expressing cells, reflecting ROS increase in the cells. Several protein chaperons such as HSP70 and GrpE-like protein co-chaperon were also identified as up-regulated proteins. Because these proteins are known to be important in the mitochondrial protein-import mechanisms, the modulated expression of these proteins may be associated with the different expressions of the identified mitochondrial proteins.

Prohibitin, a mitochondrial protein chaperon, was identified as an up-regulated protein in core-expressing cells. Prohibitin is a ubiquitously expressed and highly conserved protein that was originally determined to play a predominant role in inhibiting cell-cycle progression and cellular proliferation by attenuating DNA synthesis.[20,25] Prohibitin is present in the nucleus and interacts with transcription factors that are important in cell cycle progression. In core-expressing cells used in this study, prohibitin was also detected in the nucleus and its expression level was also higher than that in control Hepswx cells or HepG2 cells (data not shown). The growth rate of core-expressing cells, however, was similar to that of control cells (data not shown). The physiological significance of the high expression level of prohibitin in the nucleus remains to be determined, but it may be related to enhanced apoptosis by Fas ligand, as shown by Ruggieri et al.,[16] because prohibitin interacts with E2F, Rb, and p53 and modulates the transcription activity of these factors and induces apoptosis.[26,27]

Mitochondrial prohibitin acts as a protein chaperon by stabilizing newly synthesized mitochondrial translation products through direct interaction.[21] We examined the interaction between prohibitin and mitochondrially encoded subunit II of COX and found a suppressed interaction between these proteins in core-expressing cells. In addition, there are several studies that showed the association of prohibitin with the assembly of mitochondrial respiratory complex I as well as complex IV (COX).[21,28] Complex I also consists of both nuclear- and mitochondrial-DNA-encoded subunits; therefore, it is probable that the assembly and function of complex I are impaired by the core protein. We attempted to examine the interaction of prohibitin with the mitochondrial DNA-encoded subunit of complex I, but commercially available antibodies against this subunit could not detect the protein itself by immunoblotting (data not shown). With respect to the complex I function, we found a decreased complex I activity in core-expressing cells (H. Miyoshi et al., manuscript in preparation). Other groups have also shown that complex I activity is decreased in the liver of transgenic mice harboring HCV core and envelope genes[9] as well as in cultured cells.[29] From these findings, the interaction between prohibitin and the core protein may impair the function of complex I as well as complex IV, leading to an increase in ROS production. In fact, the suppression of the prohibitin function is shown to result in an increased production of ROS,[30] a phenomenon observed in core-expressing cells used in this study (Miyoshi et al., in prep.) as well as in the liver of core-gene transgenic mice.[7,8] Interestingly, Berger and Yaffe[31] showed that loss of function of prohibitin leads to an altered mitochondrial morphology, that is, the loss of the normal reticular morphology and organized mitochondrial distribution. In hepatocytes from the core-gene transgenic mice, we observed a change in morphology of mitochondria, a disappearance of the double structure of mitochondrial membranes.[2] These changes in mitochondrial morphology are somewhat different, but the dysfunction of prohibitin may be responsible for the morphological abnormality of mitochondria observed in the core-gene transgenic mice.

We concluded that prohibitin overexpression is due to increased stability induced by the interaction with the core protein. In this study we showed that prohibitin might be degraded by proteasome, although we could not detect ubiquitinated forms of prohibitin. If the degradation is mediated by ubiquitin as reported,[23] it is possible that the interaction with the core protein interferes with ubiquitin-binding and protects prohibitin from degradation by proteasome. Some posttranslational protein modifications such as phosphorylation are other possible factors for the stabilization, because prohibitin can be serine-phosphorylated[32]; however, in our examination no serine/threonine/tyrosine phosphorylation of prohibitin was detected in core-expressing cells (data not shown). Thus far, there are no studies showing that prohibitin stabilization leads to a suppressed function as a mitochondrial chaperon. Therefore, this finding is novel and noteworthy because the prohibitin expression level has been considered to be proportional to the chaperon function. Prohibitin is highly expressed in several human tumors.[33,34] In addition, a 2D-PAGE of the hepatoma cell line HCC-M identified prohibitin as a positively regulated protein.[35] In these studies, the mechanism of prohibitin overexpression was not elucidated, but considering that prohibitin is associated with the inhibition of cell proliferation, the function of prohibitin is suppressed by stabilization by some molecules in the tumor, similar to the mechanism we suggest in the current study.

In addition to HepG2 cells constitutively expressing the core protein, increased prohibitin expression levels were also found in livers of core-gene transgenic mice.

The difference in expression levels between the transgenic mice and nontransgenic littermates, however, was a little bit smaller than that in the studies of HepG2 cells. This may be due to the low expression level of the core protein in the transgenic mice compared with that in core-expressing HepG2 cells because the expression level of prohibitin was proportionally increased to that of the core protein as shown in this study (Fig. 2D). Otherwise, there might be some *in vivo* mechanism for suppressing prohibitin expression in mice.

In this study, COX subunit IV as well as II were found to interact with prohibitin (Fig. 5A). Although there are no studies demonstrating that prohibitin also works as chaperon for nuclear DNA-encoded mitochondrial proteins as far as we investigated, knockdown of prohibitin expression by siRNA led to decreases in expression levels of both nuclear (COX IV, VIb) and mitochondrial (COX I, II) DNA-encoded subunits in mitochondria (Fig. 5B and Supporting Figs. 1 and 2). We showed that COX IV interacts with prohibitin (Fig. 4), suggesting that prohibitin also works for stable expression of nuclear DNA-encoded COX IV. Degrees of decrease in COX IV and VIb expression, however, were smaller than those in I and II. Prohibitin might contribute to stabilization of COX IV and VIb by mechanism(s) other than chaperon function. Steglich et al.[36] showed that prohibitin regulates protein degradation by the m-AAA protease in mitochondria. Recently, Da Cruz et al.[37] showed that SLP-2, a member of the stomatin gene family, interacts with prohibitin and regulates the expression of mitochondrial proteins such as COX IV and ND6 of complex I encoded by nuclear DNA by AAA proteases. In view of these findings, COX IV and VIb expression in mitochondria is dependent on prohibitin but other factors may also be involved in the attainment of stable expression of these subunits. The expression levels of COX II and IV in the whole-cell lysates were not so drastic among cell samples (Fig. 5A) compared to those in the mitochondria (Fig. 5B). The reason is not clear, but it is possible that redundant proteins such as improperly folded proteins by lack of chaperons were included in the whole-cell lysates.

In summary, we analyzed mitochondrial proteins in core-expressing HepG2 cells by proteomics analysis and identified prohibitin as an up-regulated protein. The dysfunction of prohibitin induced by the core protein may lead to ROS overproduction in the mitochondrion, which plays a key role in the pathogenesis of chronic hepatitis C. The restoration of prohibitin function might be a therapeutic option for correcting the dysregulated assembly and dysfunction of mitochondrial respiratory chain complexes.

Acknowledgment: We thank S. Shinzawa, M. Yahata, and S. Yoshizaki for technical assistance.

References

1. Suzuki R, Suzuki T, Ishii K, Matsuura Y, Miyamura T. Processing and functions of Hepatitis C virus proteins. Intervirology 1999;42:145-152.
2. Moriya K, Fujie H, Shintani Y, Yotsuyanagi H, Tsutsumi T, Ishibashi K, et al. The core protein of hepatitis C virus induces hepatocellular carcinoma in transgenic mice. Nat Med 1998;4:1065-1067.
3. Naas T, Ghorbani M, Alvarez-Maya I, Lapner M, Kothary R, De Repentigny Y, et al. Characterization of liver histopathology in a transgenic mouse model expressing genotype 1a hepatitis C virus core and envelope proteins 1 and 2. J Gen Virol 2005;86:2185-2196.
4. Machida K, Cheng KT, Lai CK, Jeng KS, Sung VM, Lai MM. Hepatitis C virus triggers mitochondrial permeability transition with production of reactive oxygen species, leading to DNA damage and STAT3 activation. J Virol 2006;80:7199-7207.
5. Suzuki R, Sakamoto S, Tsutsumi T, Rikimaru A, Tanaka K, Shimoike T, et al. Molecular determinants for subcellular localization of hepatitis C virus core protein. J Virol 2005;79:1271-1281.
6. Schwer B, Ren S, Pietschmann T, Kartenbeck J, Kaehlcke K, Bartenschlager R, et al. Targeting of hepatitis C virus core protein to mitochondria through a novel C-terminal localization motif. J Virol 2004;78:7958-7968.
7. Moriya K, Nakagawa K, Santa T, Shintani Y, Fujie H, Miyoshi H, et al. Oxidative stress in the absence of inflammation in a mouse model for hepatitis C virus-associated hepatocarcinogenesis. Cancer Res 2001;61:4365-4370.
8. Okuda M, Li K, Beard MR, Showalter LA, Scholle F, Lemon SM, et al. Mitochondrial injury, oxidative stress, and antioxidant gene expression are induced by hepatitis C virus core protein. Gastroenterology 2002;122:366-375.
9. Korenaga M, Wang T, Li Y, Showalter LA, Chan T, Sun J, et al. Hepatitis C virus core protein inhibits mitochondrial electron transport and increases reactive oxygen species (ROS) production. J Biol Chem 2005;280:37481-37488.
10. Diamond DL, Jacobs JM, Paeper B, Proll SC, Gritsenko MA, Carithers RL Jr, et al. Proteomic profiling of human liver biopsies: hepatitis C virus-induced fibrosis and mitochondrial dysfunction. HEPATOLOGY 2007;46:649-657.
11. Moriya K, Yotsuyanagi H, Shintani Y, Fujie H, Ishibashi K, Matsuura Y, et al. Hepatitis C virus core protein induces hepatic steatosis in transgenic mice. J Gen Virol 1997;78(Pt 7):1527-1531.
12. Moriya K, Todoroki T, Tsutsumi T, Fujie H, Shintani Y, Miyoshi H, et al. Increase in the concentration of carbon 18 monounsaturated fatty acids in the liver with hepatitis C: analysis in transgenic mice and humans. Biochem Biophys Res Commun 2001;281:1207-1212.
13. Fujie H, Yotsuyanagi H, Moriya K, Shintani Y, Tsutsumi T, Takayama T, et al. Steatosis and intrahepatic hepatitis C virus in chronic hepatitis. J Med Virol 1999;59:141-145.
14. Cho WC. Contribution of oncoproteomics to cancer biomarker discovery. Mol Cancer 2007;6:25.
15. Lescuyer P, Strub JM, Luche S, Diemer H, Martinez P, Van Dorsselaer A, et al. Progress in the definition of a reference human mitochondrial proteome. Proteomics 2003;3:157-167.
16. Ruggieri A, Harada T, Matsuura Y, Miyamura T. Sensitization to Fas-mediated apoptosis by hepatitis C virus core protein. Virology 1997;229:68-76.
17. Okado-Matsumoto A, Fridovich I. Subcellular distribution of superoxide dismutases (SOD) in rat liver: Cu,Zn-SOD in mitochondria. J Biol Chem 2001;276:38388-38393.
18. Murakami K, Ishii K, Ishihara Y, Yoshizaki S, Tanaka K, Gotoh Y, et al. Production of infectious hepatitis C virus particles in three-dimensional cultures of the cell line carrying the genome-length dicistronic viral RNA of genotype 1b. Virology 2006;351:381-392.

19. Shevchenko A, Wilm M, Vorm O, Mann M. Mass spectrometric sequencing of proteins silver-stained polyacrylamide gels. Anal Chem 1996;68: 850-858.
20. Mishra S, Murphy LC, Murphy LJ. The prohibitins: emerging roles in diverse functions. J Cell Mol Med 2006;10:353-363.
21. Nijtmans LG, de Jong L, Artal Sanz M, Coates PJ, Berden JA, Back JW, et al. Prohibitins act as a membrane-bound chaperone for the stabilization of mitochondrial proteins. EMBO J 2000;19:2444-2451.
22. Back JW, Sanz MA, De Jong L, De Koning LJ, Nijtmans LG, De Koster CG, et al. A structure for the yeast prohibitin complex: structure prediction and evidence from chemical crosslinking and mass spectrometry. Protein Sci 2002;11:2471-2478.
23. Thompson WE, Ramalho-Santos J, Sutovsky P. Ubiquitination of prohibitin in mammalian sperm mitochondria: possible roles in the regulation of mitochondrial inheritance and sperm quality control. Biol Reprod 2003; 69:254-260.
24. Fontanesi F, Soto IC, Horn D, Barrientos A. Assembly of mitochondrial cytochrome c-oxidase, a complicated and highly regulated cellular process. Am J Physiol Cell Physiol 2006;291:C1129-C1147.
25. Mishra S, Murphy LC, Nyomba BL, Murphy LJ. Prohibitin: a potential target for new therapeutics. Trends Mol Med 2005;11:192-197.
26. Fusaro G, Dasgupta P, Rastogi S, Joshi B, Chellappan S. Prohibitin induces the transcriptional activity of p53 and is exported from the nucleus upon apoptotic signaling. J Biol Chem 2003;278:47853-47861.
27. Joshi B, Ko D, Ordonez-Ercan D, Chellappan SP. A putative coiled-coil domain of prohibitin is sufficient to repress E2F1-mediated transcription and induce apoptosis. Biochem Biophys Res Commun 2003;312:459-466.
28. Bourges I, Ramus C, Mousson de Camaret B, Beugnot R, Remacle C, Cardol P, et al. Structural organization of mitochondrial human complex I: role of the ND4 and ND5 mitochondria-encoded subunits and interaction with prohibitin. Biochem J 2004;383:491-499.
29. Piccoli C, Scrima R, Quarato G, D'Aprile A, Ripoli M, Lecce L, et al. Hepatitis C virus protein expression causes calcium-mediated mitochondrial bioenergetic dysfunction and nitro-oxidative stress. HEPATOLOGY 2007;46:58-65.
30. Theiss AL, Idell RD, Srinivasan S, Klapproth JM, Jones DP, Merlin D, et al. Prohibitin protects against oxidative stress in intestinal epithelial cells. FASEB J 2007;21:197-206.
31. Berger KH, Yaffe MP. Prohibitin family members interact genetically with mitochondrial inheritance components in Saccharomyces cerevisiae. Mol Cell Biol 1998;18:4043-4052.
32. Ross JA, Nagy ZS, Kirken RA. The PHB1/2 phosphocomplex is required for mitochondrial homeostasis and survival of human T cells. J Biol Chem 2008;283:4699-4713.
33. Coates PJ, Nenutil R, McGregor A, Picksley SM, Crouch DH, Hall PA, et al. Mammalian prohibitin proteins respond to mitochondrial stress and decrease during cellular senescence. Exp Cell Res 2001;265:262-273.
34. Asamoto M, Cohen SM. Prohibitin gene is overexpressed but not mutated in rat bladder carcinomas and cell lines. Cancer Lett 1994;83:201-207.
35. Seow TK, Ong SE, Liang RC, Ren EC, Chan L, Ou K, et al. Two-dimensional electrophoresis map of the human hepatocellular carcinoma cell line, HCC-M, and identification of the separated proteins by mass spectrometry. Electrophoresis 2000;21:1787-1813.
36. Steglich G, Neupert W, Langer T. Prohibitins regulate membrane protein degradation by the m-AAA protease in mitochondria. Mol Cell Biol 1999; 19:3435-3442.
37. Da Cruz S, Parone PA, Gonzalo P, Bienvenut WV, Tondera D, Jourdain A, et al. SLP-2 interacts with prohibitins in the mitochondrial inner membrane and contributes to their stability. Biochim Biophys Acta 2008;1783: 904-911.

Hepatitis B Virus X Protein Shifts Human Hepatic Transforming Growth Factor (TGF)-β Signaling from Tumor Suppression to Oncogenesis in Early Chronic Hepatitis B

Miki Murata,[1] Koichi Matsuzaki,[1] Katsunori Yoshida,[1] Go Sekimoto,[1] Yoshiya Tahashi,[1] Shigeo Mori,[1] Yoshiko Uemura,[2] Noriko Sakaida,[2] Junichi Fujisawa,[3] Toshihito Seki,[1] Kazuki Kobayashi,[4] Koutaro Yokote,[4] Kazuhiko Koike,[5] and Kazuichi Okazaki[1]

Hepatitis B virus X (HBx) protein is suspected to participate in oncogenesis during chronic hepatitis B progression. Transforming growth factor β (TGF-β) signaling involves both tumor suppression and oncogenesis. TGF-β activates TGF-β type I receptor (TβRI) and c-Jun N-terminal kinase (JNK), which differentially phosphorylate the mediator Smad3 to become C-terminally phosphorylated Smad3 (pSmad3C) and linker-phosphorylated Smad3 (pSmad3L). Reversible shifting of Smad3-mediated signaling between tumor suppression and oncogenesis in HBx-expressing hepatocytes indicated that TβRI-dependent pSmad3C transmitted a tumor-suppressive TGF-β signal, while JNK-dependent pSmad3L promoted cell growth. We used immunostaining, immunoblotting, and *in vitro* kinase assay to compare pSmad3L- and pSmad3C-mediated signaling in biopsy specimens representing chronic hepatitis, cirrhosis, or hepatocellular carcinoma (HCC) from 90 patients chronically infected with hepatitis B virus (HBV) with signaling in liver specimens from HBx transgenic mice. In proportion to plasma HBV DNA levels, early chronic hepatitis B specimens showed prominence of pSmad3L in hepatocytic nuclei. HBx-activated JNK/pSmad3L/c-Myc oncogenic pathway was enhanced, while the TβRI/pSmad3C/p21^{WAF1} tumor-suppressive pathway was impaired as human and mouse HBx-associated hepatocarcinogenesis progressed. Of 28 patients with chronic hepatitis B who showed strong oncogenic pSmad3L signaling, six developed HCC within 12 years; only one of 32 patients showing little pSmad3L developed HCC. In contrast, seven of 30 patients with little Smad3C phosphorylation developed HCC, while no patient who retained hepatocytic tumor-suppressive pSmad3C developed HCC within 12 years. *Conclusion:* HBx shifts hepatocytic TGF-β signaling from the tumor-suppressive pSmad3C pathway to the oncogenic pSmad3L pathway in early carcinogenic process. Hepatocytic pSmad3L and pSmad3C assessment in HBV-infected liver specimens should prove clinically useful for predicting risk of HCC. (HEPATOLOGY 2009;49:1203-1217.)

Hepatocellular carcinoma (HCC) is the fifth most common cancer worldwide and one of the most deadly, causing approximately 600,000 deaths yearly.[1] The overall incidence of HCC continues to rise, especially in western Europe and the United States.[2] During the past 20 years, striking advances have enhanced our understanding of HCC. More than 85% of HCC cases are related to known hepatitis B virus (HBV) and hepatitis C virus (HCV).

Abbreviations: Ab, antibody; HBV, hepatitis B virus; HBx, hepatitis B virus X; HCC, hepatocellular carcinoma; HCV, hepatitis C virus; HSC, hepatic stellate cells; IgG, immunoglobulin G; JNK, c-Jun N-terminal kinase; PPM1A, protein phosphatase magnesium 1A; pSmad3C, C-terminally phosphorylated Smad3; pSmad3L, linker-phosphorylated Smad3; SCP1-3, small C-terminal domain phosphatase 1-3; TGF-β, transforming growth factor β; TβRI, TGF-β type I receptor; TβRII, TGF-β type II receptor.

From the Departments of [1]Gastroenterology and Hepatology, [2]Surgical Pathology, and [3]Microbiology, Kansai Medical University, Osaka, Japan; the [4]Department of Clinical Cell Biology, Chiba University Graduate School of Medicine, Chiba, Japan; and the [5]Department of Infectious Diseases, Internal Medicine, Graduate School of Medicine, University of Tokyo, Tokyo, Japan.

Received March 19, 2008; accepted November 25, 2008.

Supported by the Ministry of Education, Science, and Culture of Japan (K. M.).

A strong correlation between chronic HBV infection and HCC occurrence has long been apparent according to epidemiologic evidence and the finding of integrated HBV DNA sequences in virtually all HBV-related HCC.[3] Hepatitis B virus X (HBx) oncoprotein has been implicated in HBV-mediated hepatocarcinogenesis,[4,5] and persistent high-level expression of HBx protein in transgenic mouse liver results in hyperplasia leading to HCC, with no preceding inflammation.[6] Although HBx does not bind DNA directly, HBx activates Ras/mitogen-activated protein kinase pathways including extracellular signal-regulated kinase and c-Jun N-terminal kinase (JNK),[7] resulting in tumor cell growth and survival.

Transforming growth factor β (TGF-β) can inhibit epithelial cell growth, acting as a tumor suppressor. During carcinogenesis, however, cancer cells gain advantage by selective reduction of the tumor-suppressive activity of TGF-β together with augmentation of its oncogenic activity.[8] This led us to hypothesize that alterations in the TGF-β signal transduction pathway could be involved in the development of HCC in long-standing HBV infection.

Smads are central mediators of signals from the receptors for TGF-β superfamily members to the nucleus.[9] Smads are modular proteins with conserved Mad-homology 1, intermediate linker, and Mad-homology 2 domains.[10] The catalytically active TGF-β type I receptor (TβRI) phosphorylates the C-terminal serine residues of receptor-activated Smads, which include Smad2 and the highly related protein Smad3. The linker domain can undergo regulatory phosphorylation by other kinases including mitogen-activated protein kinases and cyclin-dependent kinases.[11-14] In contrast to the clearly activating role of the C-terminal phosphorylation events, the regulation of Smad activity by phosphorylation of the linker region is complex. Linker phosphorylation of Smad2 during human colorectal carcinogenesis results in cytoplasmic retention of Smad2 and inhibition of tumor-suppressive TGF-β signaling.[11,15] However, Smad3 phosphorylated at the linker region (pSmad3L) is localized predominantly to cell nuclei in actively growing Ki-67–immunoreactive colon cancer with distant metastasis.[15] Reversible shifting of Smad-dependent signaling between tumor suppression and oncogenesis in hyperactive Ras-expressing cells indicates that Smad3 phosphorylated at the C-terminal region (pSmad3C) transmits a tumor-suppressive TGF-β signal, whereas oncogenic activities such as cell proliferation and invasion are promoted by the pSmad3L pathway.[16] In addition, Roberts' group[17] has recently reported that Smad3 is critical for Ras/JNK-mediated transformation. Taken together, these findings indicate that oncogenic TGF-β signaling results from the functional collaboration of Ras and Smad3 rather than from Ras-mediated inhibition of the Smad3 pathway. Linker phosphorylation of Smad3 indirectly inhibits C-terminal phosphorylation, minimizing tumor-suppressive pSmad3C signaling.[16] Notably, pSmad3L-mediated signaling in activated hepatic stellate cells (HSCs) promotes liver fibrosis by stimulating extracellular matrix deposition.[13,18]

The role of HBV and HCV in tumor formation appears to be complex and may involve both direct and indirect mechanisms.[19] Integration of HBV DNA into the host genome occurs at early steps of clonal tumor expansion. Alternatively, chronic liver inflammation and hepatic regeneration induced by host cellular immune responses can increase the risk of HCC development. During progression of HCV-related chronic liver disorders, hepatocytes affected by chronic inflammation undergo a transition from the tumor-suppressive pSmad3C pathway to the JNK/pSmad3L pathway.[20] Our present studies extend the previous observations to HBV-related hepatocarcinogenesis. We study Smad3 phosphorylation profiles in HBV-infected human liver and HBx transgenic mouse liver, concluding that HBx oncoprotein in early stages of chronic hepatitis B contributes directly to hepatocarcinogenesis by shifting hepatocytic Smad3-mediated signaling from tumor suppression to oncogenesis.

Patients and Methods

Patients, Follow-up, and Detection of HCC. Ninety patients with HBV-related chronic liver disease underwent liver biopsy at the Department of Gastroenterology and Hepatology of Kansai Medical University Hospital between 1992 and 1994. All patients were seropositive for hepatitis B surface antigen (Abbott Laboratories, North Chicago, IL) and were seronegative for anti-HCV antibody (Ortho Diagnostics, Tokyo, Japan). Patients included 70 with chronic hepatitis, 10 with cir-

Address reprint requests to: Koichi Matsuzaki, M.D., Departments of Gastroenterology and Hepatology, Kansai Medical University, 10-15 Fumizonocho, Moriguchi, Osaka, 570-8507, Japan. E-mail: matsuzak@takii.kmu.ac.jp; fax: (81)-6-6996-4874.

Published online in Wiley InterScience (www.interscience.wiley.com).
DOI 10.1002/hep.22765
Potential conflict of interest: Nothing to report.
Additional Supporting Information may be found on the online version of this article.

rhosis, and 10 with HCC. Sixty of the chronic hepatitis patients were enrolled in a program for early diagnosis of HCC; the other 10 were lost to follow-up. HBV DNA (Roche Diagnostics, Tokyo, Japan) and hepatitis B envelope antigen (Abbott Laboratories) were measured at the time of liver biopsy. During the surveillance period, patients were followed up with abdominal ultrasonography and plasma alpha-fetoprotein determinations every 3 to 6 months. We also made a random choice of 20 chronic hepatitis B specimens with little fibrosis (F1) and little inflammation (A1) from the liver biopsy specimens of the patients showing high plasma HBV DNA levels.

Necroinflammatory activity and fibrotic stage were graded histologically according to the classification of Desmet and colleagues.[21] We counted and scored pSmad3, HBx, and c-Myc positivity in hepatocytes as follows: 0, no positivity; 1, <25%; 2, 25% to 50%; 3, 50% to 75%; 4, >75%.[20] Written informed consent was obtained from each patient according to the Helsinki Declaration. We also obtained approval for this study from our institutional ethics committee.

Reverse-Transcription Polymerase Chain Reaction. Reverse-transcription polymerase chain reaction of TGF-β type II receptor (TβRII), Smad2, and Smad4 genes was performed as described.[15]

Domain-Specific Antibodies Against the Phosphorylated Smad3. Two polyclonal anti-phospho–Smad3 sera—α pSmad3L (Ser 208/213) and α pSmad3C (Ser 423/425)—were raised against the phosphorylated linker and C-terminal regions of Smad3 by immunization of rabbits with synthetic peptides. Relevant antisera were affinity-purified using phosphorylated peptides as described.[13]

Transgenic Animals. HBx transgenic mice were derived by microinjection of a 1151-bp HBV DNA fragment containing the HBx gene with its own regulatory elements and polyadenylation signal into fertilized eggs of CD-1 mice. An independent line (H9) was derived from founders.[6]

Immunohistochemical and Immunofluorescence Analyses. Immunohistochemical and immunofluorescence analyses were performed as described.[18] Primary antibodies (Abs) used in this study included mouse monoclonal anti-HBx Ab (2 μg/mL; Abcam, Cambridge, UK), mouse monoclonal anti-c-Myc Ab (10 μg/mL; Santa Cruz Biotechnology, Santa Cruz, CA), and mouse monoclonal anti-$p21^{WAF1}$ Ab (0.5 μg/mL; DAKO, Glostrup, Denmark), in addition to the affinity-purified rabbit polyclonal anti-pSmad3L (2 μg/mL) and anti-pSmad3C (0.5 μg/mL) as described above. Anti-pSmad3C Ab cross-reacted weakly with C-terminally phosphorylated Smad2: to block binding of anti-pSmad3C Ab to phosphorylated domains in Smad2, anti-pSmad3C Ab was adsorbed with 1 μg/mL C-terminally phosphorylated Smad2 peptide.

For immunohistochemical analyses, sections exposed to primary Abs were then incubated with peroxidase-labeled polymer conjugated to goat anti-mouse or anti-rabbit immunoglobulin G (IgG) (DAKO). Finally, sections were developed with 3,3'-diaminobenzidine tetrahydrochloride (DAB; Vector Laboratories, Burlingame, CA), counterstained with Mayer's hematoxylin (Merck, Darmstadt, Germany), and mounted under coverslips.

For double-labeling immunofluorescence analyses, sections exposed to a pair of primary Abs (rabbit plus mouse) were then incubated in a 1:500 dilution of goat anti-rabbit IgG conjugated with a red fluorophore (Alexa Fluor 594; Molecular Probes, Eugene, OR) and goat anti-mouse IgG conjugated with a green fluorophore (Alexa Fluor 488; Molecular Probes). Images were obtained with a fluorescence microscope (Carl Zeiss Microimaging, Oberkochen, Germany).

Immunoprecipitation and Immunoblotting. pSmad3L and pSmad3C immunoblots on Smad3 immunoprecipitates of cell extracts from frozen tissues representing either HCC or underlying liver diseases were performed as described.[20]

In Vitro *Kinase Assay.* *In vitro* kinase assay was performed as described.[12]

Statistical Analyses. The Kaplan-Meier method was used to determine the cumulative probability of appearance of HCC during the 12-year follow-up period. HCC occurrence curves were compared between patients with abundant (scores 3 to 4) and those with sparse (scores 0 to 2) Smad3L/C phosphorylation, by means of the log-rank test. For continuous variables, the optimal cutoff threshold for defining groups was established using receiver operating characteristics curves. All parameters with P values less than 0.10 in the univariate analysis were selected for multivariate analysis, which was performed using the Cox proportional hazards model.[22] P values less than 0.05 were considered significant. The Mann-Whitney U test was used to identify significant differences in hepatocytic pSmad3L and pSmad3C positivity among fibrotic stages.

Results

Two Distinct Hepatocytic Smad3 Signaling Pathways in Human Chronic Hepatitis B: pSmad3L- and pSmad3C-Dominant Types. We initially analyzed mutations of TβRII, Smad2, and Smad4 genes in 10 HCC and six cirrhotic liver samples, finding no mutations in

Table 1. Clinicopathologic Features, Smad3L/C Phosphorylation, and HBx and c-Myc Positivities in Specimens from Patients with HBV-Related Chronic Liver Disease

		Fibrotic Stage*				
	Nomal	F1	F2	F3	F4	HCC
Patients, n	2	20	27	23	10	10
Sex (male/female), n	2/0	13/7	19/8	17/6	5/5	10/0
Age (years), mean ± SD	57.0 ± 9.9	35.5 ± 14.3	34.3 ± 13.9	43.1 ± 13.7	59.6 ± 7.6	54.0 ± 15.1
pSmad3L staining, n†						
0	2	0	0	0	0	0
1	0	8	6	2	1	0
2	0	6	6	7	1	0
3	0	3	11	11	2	5
4	0	3	4	3	6	5
pSmad3C staining, n†						
0	0	0	0	0	0	0
1	0	0	4	4	2	4
2	0	4	9	12	7	3
3	2	11	7	5	1	3
4	0	5	7	2	0	0
Activity, n*						
A0	2	1	0	0	0	0
A1	0	17	6	1	0	1
A2	0	2	19	11	3	7
A3	0	0	2	11	7	2
HBx staining, n†						
0	2	0	0	0	1	1
1	0	6	5	3	2	3
2	0	7	11	8	3	3
3	0	3	7	6	2	2
4	0	4	4	6	2	1
c-Myc staining, n†						
0	2	0	0	0	0	0
1	0	2	4	1	1	0
2	0	9	10	8	3	1
3	0	6	8	8	3	3
4	0	3	5	6	3	6
Histology of HCC (well/moderate)‡						6/4
TNM stage (I/II/III/IV)ʃ						4/4/2/0
Size of tumor (cm), mean ± SD						2.2 ± 0.3
AST (IU/L), mean ± SD	22.5 ± 3.5	68.6 ± 56.1	92.8 ± 65.8	79.7 ± 51.8	82.0 ± 53.1	71.0 ± 36.4
ALT (IU/L), mean ± SD	24.0 ± 2.8	104 ± 83.5	141 ± 97.5	84.5 ± 83.1	68.2 ± 52.3	59.1 ± 32.2
Platelet count (× 10^9/L), mean ± SD	25.0 ± 4.2	17.1 ± 3.6	15.8 ± 4.9	14.1 ± 7.1	9.7 ± 6.7	9.0 ± 3.7
AFP (ng/mL), mean ± SD	2.1 ± 1.3	6.8 ± 4.6	14.8 ± 12.2	66.2 ± 138	132 ± 208	164 ± 184

Abbreviations: AFP, alpha-fetoprotein; ALT, alanine aminotransferase; AST, aspartate aminotransferase; pSmad3L, linker-phosphorylated Smad3; pSmad3C, C-terminally phosphorylated Smad3; SD, standard deviation; TNM, tumor-node-metastasis.

*Necroinflammatory activity and fibrotic stage are determined histologically according to Desmet's classification.

†Hepatocytic Smad3 phosphorylation is scored as follows: 0, no phosphorylation; 1, <25% Smad3 phosphorylation; 2, 25% to 50% Smad3 phosphorylation; 3, 50% to 75% Smad3 phosphorylation; 4, >75% Smad3 phosphorylation. Extent of HBx and c-Myc expression is indicated as that of pSmad3L positivity.

‡Histological grading of HCC is classified according to the criteria of the International Working Party.

ʃTNM is classified by the International Union Against Cancer and American joint Committee on Cancer.

any sample. This confirms the low probability of mutations in HCC tissues, which has been reported recently.[23]

To investigate domain-specific phosphorylation mediating Smad3 signaling *in vivo*, we generated two Abs specific to each phosphorylation site, and determined the distribution of pSmad3L and pSmad3C in chronic hepatitis B and C specimens. Table 1 shows clinical background and positivity for pSmad3L and pSmad3C in 90 patients with HBV-related chronic liver diseases. We also studied HCC occurrence over 12 years in 60 patients with chronic hepatitis B who were enrolled in a program for early diagnosis of HCC (Table 2). We recently reported that Smad3 was phosphorylated at the linker region, particularly in groups of hepatocytes adjoining collagen fibers in portal tracts in chronic hepatitis C.[20] In contrast, the distribution of pSmad3L and pSmad3C in chronic

Table 2. Clinicopathologic Features, Smad3L/C Phosphorylation, and HCC Incidence in Specimens from Patients with HBV-Related Chronic Hepatitis

Patient No.	Sex	Age	Incidence of HCC	pSmad3L Staining*	pSmad3C Staining*	Fibrotic Stage†	Inflammatory Activity†	HBV DNA (log copies/mL)	HBeAg
1	M	62	○	4	2	3	3	5.4	+
2	F	44	○	4	2	2	2	5.5	−
3	M	22	○	4	2	2	2	5.2	−
4	F	20		4	4	3	3	3.0	−
5	M	43		4	4	2	2	4.5	−
6	M	30		4	2	2	3	4.0	−
7	M	30		4	2	2	3	5.6	−
8	M	65	○	3	2	3	3	4.0	+
9	F	56	○	3	2	3	2	3.7	+
10	M	52	○	3	1	1	1	6.4	−
11	F	40		3	1	1	1	6.9	−
12	M	44		3	1	3	3	5.1	−
13	M	45		3	1	3	3	3.8	−
14	M	28		3	2	3	1	3.0	−
15	M	60		3	2	3	2	2.8	−
16	M	44		3	2	3	3	5.2	+
17	M	44		3	2	3	3	3.2	+
18	M	44		3	2	3	3	4.4	−
19	F	26		3	2	2	1	4.9	−
20	M	20		3	2	2	1	2.9	+
21	M	59		3	2	2	2	4.4	−
22	M	43		3	3	2	2	3.2	+
23	M	29		3	3	3	2	6.2	−
24	M	29		3	3	3	2	3.0	−
25	M	25		3	4	1	1	3.5	−
26	F	33		3	4	2	2	4.6	+
27	M	19		3	3	3	2	5.6	−
28	M	63		3	4	2	2	5.1	−
29	M	52	○	2	1	3	2	3.7	−
30	M	44		2	2	3	3	5.2	−
31	M	29		2	2	3	2	3.9	+
32	F	46		2	4	3	3	3.2	−
33	M	25		2	2	1	2	5.0	−
34	F	23		2	3	1	1	2.1	−
35	F	31		2	3	2	2	3.9	+
36	F	26		2	3	1	1	2.4	−
37	M	35		2	3	1	1	5.6	−
38	M	20		2	3	2	1	3.2	+
39	F	56		2	3	3	2	5.1	+
40	F	36		2	3	3	2	2.6	−
41	F	25		2	3	2	1	5.1	−
42	F	23		2	4	2	1	3.5	−
43	F	41		2	4	1	1	2.0	+
44	M	29		2	4	2	2	4.5	−
45	M	31		2	4	1	1	5.9	+
46	M	42		2	1	2	2	3.7	−
47	M	24		1	1	2	2	3.9	+
48	M	28		1	2	3	2	3.8	−
49	F	11		1	2	2	2	3.0	+
50	M	40		1	1	2	2	3.2	−
51	M	37		1	2	2	2	3.0	−
52	F	10		1	2	2	2	2.3	−
53	M	16		1	3	1	1	5.1	−
54	M	41		1	3	1	1	4.3	−
55	M	40		1	3	1	1	2.2	−
56	M	53		1	3	1	1	2.7	−
57	M	27		1	3	1	1	4.6	−
58	M	53		1	4	1	1	3.3	−
59	M	30		1	4	2	2	2.1	−
60	F	22		1	4	1	0	3.7	−

Abbreviations: F, female; HBeAg, hepatitis B e antigen; HBV, hepatitis B virus; HCC, hepatocellular carcinoma; M, male; pSmad3C, C-terminally phosphorylated Smad3; pSmad3L, linker-phosphorylated Smad3.

*Hepatocytic Smad3 phosphorylation is scored as follows: 0, no phosphorylation; 1, <25% Smad3 phosphorylation; 2, 25% to 50% Smad3 phosphorylation; 3, 50% to 75% Smad3 phosphorylation; 4, >75% Smad3 phosphorylation.

†Necroinflammatory activity and fibrotic stage are determined histologically according to Desmet's classification.

hepatitis B specimens was divided into two distinct patterns. In one liver specimen with moderate fibrosis and inflammation from patient 2 in Table 2 who was diagnosed with HCC 9 years later, intense pSmad3L immunostaining was present in the nuclei of all hepatocytes throughout the liver lobules; C-terminal phosphorylation of Smad3 was strongly suppressed in hepatocytic nuclei (Fig. 1A and Supplementary Fig. 1). In another specimen with similar fibrotic stage and necroinflammatory activity from patient 44 in Table 2 who had not developed HCC, many hepatocytes retained phosphorylation at Smad3C but showed scarce phosphorylation at Smad3L (Fig. 1B). Among 37 patients with chronic hepatitis B who had strong pSmad3L positivity, 24 patients showed little Smad3C phosphorylation, and only 13 patients showed abundant Smad3C phosphorylation (64.9% versus 35.1% [$P = 0.03$]) (Table 3). In contrast, 22 patients with little Smad3L phosphorylation (scores 0 to 2) versus only 13 patients with abundant Smad3L phosphorylation (scores 3 to 4) showed strong pSmad3C positivity (62.9% versus 37.1% [$P = 0.04$]). Because the extent of Smad3L phosphorylation increased as fibrotic stage and necroinflammatory activity progressed in chronic hepatitis C, Smad3L showed little phosphorylation in early chronic hepatitis C.[20] In contrast, degree of linker phosphorylation of Smad3 in hepatocytic nuclei remained high (staining scored as 3 or 4) in 21 of 47 patients with chronic hepatitis B (F1 to F2) (Fig. 1C). These results indicate differential mechanisms of HBV- and HCV-

Table 3. Correlation Between pSmad3L and pSmad3C in Chronic Hepatitis B Specimens

	pSmad3C Positivity *		
	Low (1 and 2)	High (3 and 4)	Total
pSmad3L positivity *			
Low (1 and 2)	11	22	33
High (3 and 4)	24	13	37
Total	35	35	70

Abbreviations: pSmad3C, C-terminally phosphorylated Smad3; pSmad3L, linker-phosphorylated Smad3.

*Hepatocytic Smad3 phosphorylation is scored as follows: 0, no phosphorylation; 1, <25% Smad3 phosphorylation; 2, 25% to 50% Smad3 phosphorylation; 3, 50% to 75% Smad3 phosphorylation; 4, >75% Smad3 phosphorylation.

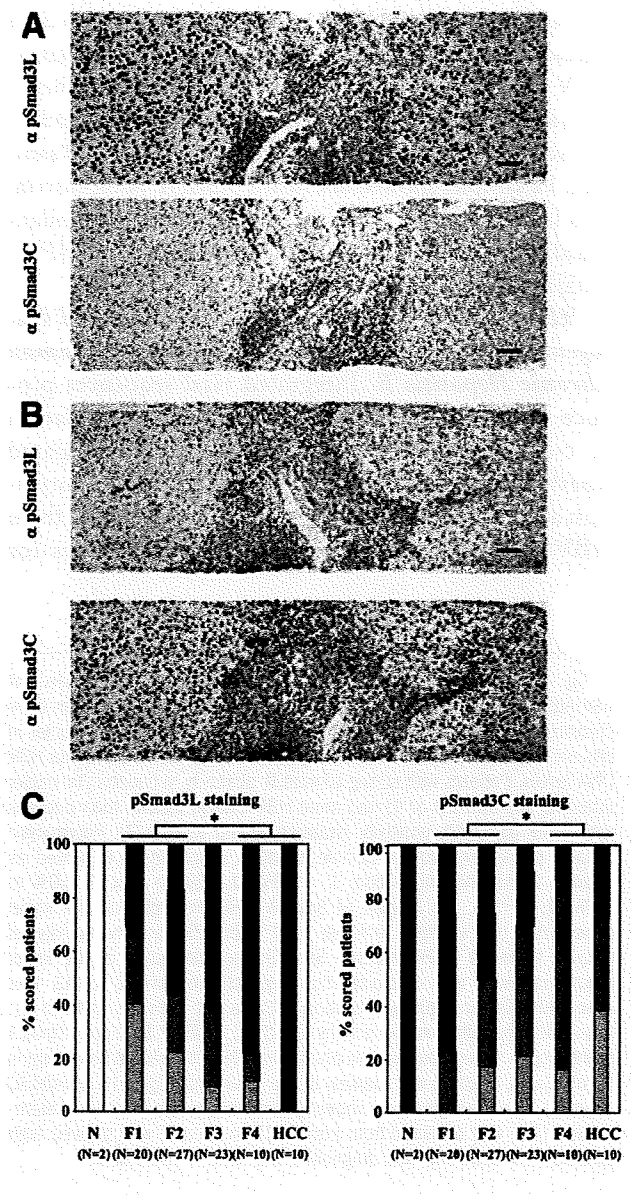

COLOR

Fig. 1. Two distinct hepatocytic Smad3 signaling pathways in early chronic hepatitis B: pSmad3L- and pSmad3C-dominant types. (A) Smad3 in the nuclei of hepatocytes was phosphorylated sparsely at the C-terminal region (α pSmad3C column) but intensely at the linker region (α pSmad3L column). The liver specimen showing moderate fibrosis and inflammation was obtained from patient 2 in Table 2 diagnosed with HCC 9 years later. Bar = 50 μm. (B) In patient 44 in Table 2 who had not developed HCC, hepatocytes retained phosphorylation at Smad3C (α pSmad3C column) but showed little phosphorylation at Smad3L (α pSmad3L column). The specimen showed degrees of fibrosis and necroinflammatory activity similar to those in (A). Formalin-fixed, paraffin-embedded liver sections were stained with anti-pSmad3L Ab (α pSmad3L column) and anti-pSmad3C Ab (α pSmad3C column). The pSmad3C section was paired with an adjacent section stained using anti-pSmad3L Ab. Abs were then bound by goat anti-rabbit IgG conjugated with peroxidase-labeled polymer. Peroxidase activity was detected with 3,3'-diaminobenzidine tetrahydrochloride. All sections were counterstained with hemotoxylin (blue). Brown color indicates specific Ab reactivity. Bar = 50 μm. (C) Degrees of Smad3 phosphorylation were stable in hepatocytic nuclei in early chronic hepatitis B specimens (F1 to F2), whereas pSmad3L increased and pSmad3C decreased as chronic hepatitis B (F3) progressed through cirrhosis to HCC. Smad3 phosphorylation in hepatocytes did not change between F1 and F2 stages. Phosphorylation of Smad3L and Smad3C in hepatocytes of cirrhotic liver (F4) and HCC was greater and less than that in livers with grade F1 and F2 fibrosis, respectively. Extent of Smad3 phosphorylation: □, 0; □, 1; ▒, 2; ▓, 3; ■, 4. *$P < 0.05$.

associated carcinogenesis, especially in the early stages of chronic hepatitis.

pSmad3L Prominence in Hepatocytic Nuclei in Proportion to Plasma HBV DNA Levels. Because HCC risk is related to plasma HBV DNA levels and chronic inflammation,[24] we next investigated the correlation of hepatocytic pSmad3L positivity with plasma HBV DNA levels and necroinflammatory activity in chronic hepatitis B patients (Fig. 2). Positivity of hepatocytic nuclei for pSmad3L in chronic hepatitis B specimens gradually increased in proportion to amounts of HBV DNA. Sixteen sera samples of 35 patients with abundant Smad3L phosphorylation (scores 3 to 4) but only seven sera samples of 35 patients with little Smad3L phosphorylation (scores 0 to 2) contained more than 5.0 log copies/mL (45.7% versus 20.0% [$P = 0.02$]) (Fig. 2A). However, 23 of 35 chronic hepatitis B patients with abundant Smad3L phosphorylation and 22 of 35 patients with little Smad3L phosphorylation showed a high level of inflammatory activity (A 2 to 3) (65.7% versus 62.9% [$P = 0.80$]) (Fig. 2B). These results indicated that HBV itself could up-regulate the hepatocytic phosphorylation at Smad3L, but inflammation could not strongly affect linker phosphorylation.

To further confirm the direct effects of HBV, besides chronic inflammation, on phosphorylation at Smad3L in early chronic hepatitis B, we examined the degrees of pSmad3L and pSmad3C in a group of patients with little fibrosis (F1), little inflammation (A1), and high plasma HBV DNA. Smad3L was highly phosphorylated in hepatocytic nuclei, whereas the phosphorylation at Smad3C was suppressed (Fig. 2C). Of 20 chronic hepatitis B samples, 12 samples showed abundant Smad3L phosphorylation (scores 3 to 4), but only five samples had abundant Smad3C phosphorylation (60.0% versus 25.0% [$P = 0.03$]) (Table 4).

HBx Protein Involvement in c-Myc–Mediated Oncogenic Activity via the pSmad3L Pathway in Human Chronic Hepatitis B. Integrated viral sequences produce HBx protein, which brings about up-regulation of c-Myc oncoprotein.[25] We therefore investigated whether HBx protein affected Smad3L phosphorylation and expression of c-Myc in biopsy specimens from HBV-infected livers by immunostaining sections for

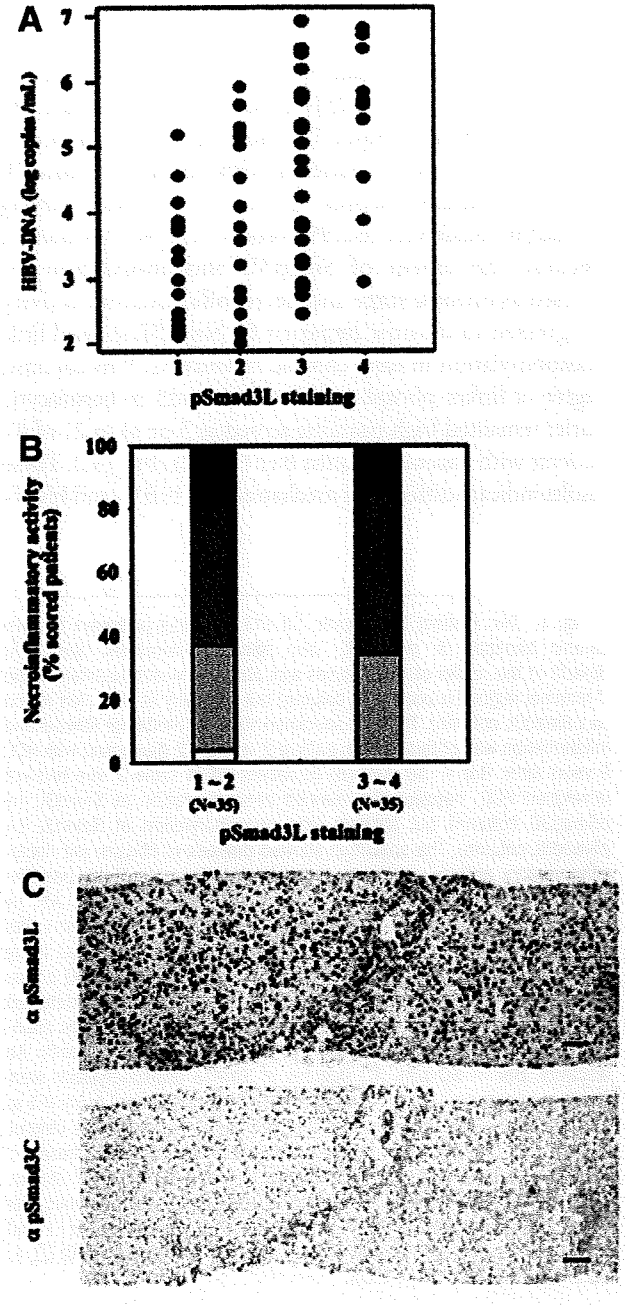

Fig. 2. In proportion to plasma HBV DNA levels, JNK-dependent pSmad3L became prominent in the nuclei of hepatocytes in human early chronic hepatitis B. (A) Positivity for pSmad3L in hepatocytic nuclei in chronic hepatitis B specimens was greater in proportion to plasma HBV DNA levels. Patients with strong pSmad3L positivity in hepatocytic nuclei (staining scored as 3 or 4) had more HBV DNA in plasma than patients with weak pSmad3L positivity (staining scored as 0 to 2). Hepatocytic Smad3 phosphorylation in chronic hepatitis B specimens is scored as follows: 0, no phosphorylation; 1, <25%; 2, 25% to 50%; 3, 50% to 75%; 4, >75%. (B) Degree of Smad3 phosphorylation at the linker region did not strongly correlate with necroinflammatory activity of chronic hepatitis B. Hepatocytic Smad3 phosphorylation at the linker region in livers with necroinflammatory activities of A2 to A3 was essentially similar to phosphorylation in those with activities of A0 to A1. Extent of necroinflammatory activity: □, 0; □, 1; ■, 2; ■, 3. (C) Smad3 in the nuclei of hepatocytes was phosphorylated intensely at linker region (α pSmad3L column) but sparsely at the C-terminal region (α pSmad3C column). The liver specimen showing minimal fibrosis (F1) and inflammation (A1) was obtained from patient 10 in Table 2 who showed high plasma HBV DNA and was diagnosed with HCC 4 years later.

Table 4. Clinicopathologic Features, Smad3L/C Phosphorylation, and Plasma HBV DNA Levels in Specimens from Patients with Early Chronic Hepatitis B

Patient No.	Sex	Age	pSmad3L staining*	pSmad3C staining*	Fibrotic Stage†	Inflammatory Activity†	HBV DNA (log copies/mL)
1	M	46	4	2	1	1	5.6
2	M	45	4	2	1	1	5.4
3	F	38	3	1	1	1	6.2
4	F	49	3	1	1	1	5.2
5	F	52	3	1	1	1	6.1
6	F	40	3	2	1	1	5.8
7	F	28	3	2	1	1	5.6
8	M	38	3	2	1	1	5.5
9	M	44	3	2	1	1	5.3
10	F	40	3	2	1	1	5.4
11	M	55	3	2	1	1	5.1
12	F	43	3	3	1	1	5.8
13	M	34	2	1	1	1	5.2
14	M	28	1	1	1	1	5.2
15	F	35	1	2	1	1	5.1
16	M	30	1	2	1	1	5.3
17	M	45	1	3	1	1	5.2
18	M	38	1	4	1	1	5.6
19	M	54	1	4	1	1	5.2
20	M	48	1	4	1	1	5.4

Abbreviations: F, female; HBV, hepatitis B virus; M, male; pSmad3C, C-terminally phosphorylated Smad3; pSmad3L, linker-phosphorylated Smad3.

*Hepatocytic Smad3 phosphorylation is scored as follows: 0, no phosphorylation; 1, <25% Smad3 phosphorylation; 2, 25% to 50% Smad3 phosphorylation; 3, 50% to 75% Smad3 phosphorylation; 4, >75% Smad3 phosphorylation.

†Necroinflammatory activity and fibrotic stage are determined histologically according to Desmet's classification.

pSmad3L, paired with sections immunostained for HBx and c-Myc.

In specimens from patient 3 in Table 2 with chronic hepatitis B, pSmad3L, HBx, and c-Myc were distributed in hepatocytes throughout liver lobules (Fig. 3A and Supplementary Fig. 2). Double immunofluorescence studies in chronic hepatitis B specimens confirmed that pSmad3L was colocalized in HBx- and c-Myc–immunoreactive hepatocytes (Fig. 3B). HBx and c-Myc expression increased in hepatocytes of hepatitis B specimens as Smad3 showed more phosphorylation at the linker region (Fig. 3C).

Increased JNK/pSmad3L/c-Myc Oncogenic Signaling and Impaired pSmad3C/p21 ^{WAF1} Tumor-Suppressive Signaling as Chronic Hepatitis B Progresses From Cirrhosis to HCC. We further investigated tumor-suppressive and oncogenic Smad3 signaling in biopsy specimens during HBV-related hepatocarcinogenesis by staining sections using anti-pSmad3L Ab and anti-pSmad3C Ab, paired with sections stained for anti–c-Myc Ab and anti-p21^{WAF1} Ab. Although pSmad3L accelerates tumor growth by up-regulating c-Myc, pSmad3C participates in tumor suppression by up-regulating p21^{WAF1} transcription.[16, 20]

In specimens from a patient with chronic hepatitis B, the distribution of pSmad3L fit well with the pattern shown by c-Myc immunolabeling (Fig. 4A, chronic hepatitis panel): both were strong in hepatocytes throughout liver lobules. Linker phosphorylation and c-Myc staining increased further as chronic liver disease progressed through cirrhosis to HCC (Fig. 4A, cirrhosis and HCC panels).

Distribution of pSmad3C resembled the pattern obtained by p21^{WAF1} staining in chronic hepatitis B specimens (Fig. 4B, chronic hepatitis panel). As with pSmad3C distribution, hepatocytes showed increased p21^{WAF1} staining in nuclei. In contrast to intense staining for pSmad3L and c-Myc, pSmad3C and p21^{WAF1} staining decreased in hepatocytic nuclei in cirrhotic liver (Fig. 4B, cirrhosis panel). Nuclear pSmad3C and p21^{WAF1} immunostaining showed only a scattered distribution throughout HCC specimens (Fig. 4B, HCC panel). Semiquantitative analyses of positivity for pSmad3L, pSmad3C, and c-Myc in HBV-related chronic liver disease showed increasing pSmad3L/c-Myc and decreasing pSmad3C as chronic hepatitis B progressed from cirrhosis (F4) to HCC (Table 1).

We next quantified the extent of phosphorylation at Smad3L and Smad3C by immunoblotting with domain-specific Abs against phosphorylated Smad3 in tissue samples representing various stages of HBV-related chronic liver disorders. The linker region of Smad3 showed very little phosphorylation in normal liver (Fig. 4C, α pSmad3L panel). Remarkable up-

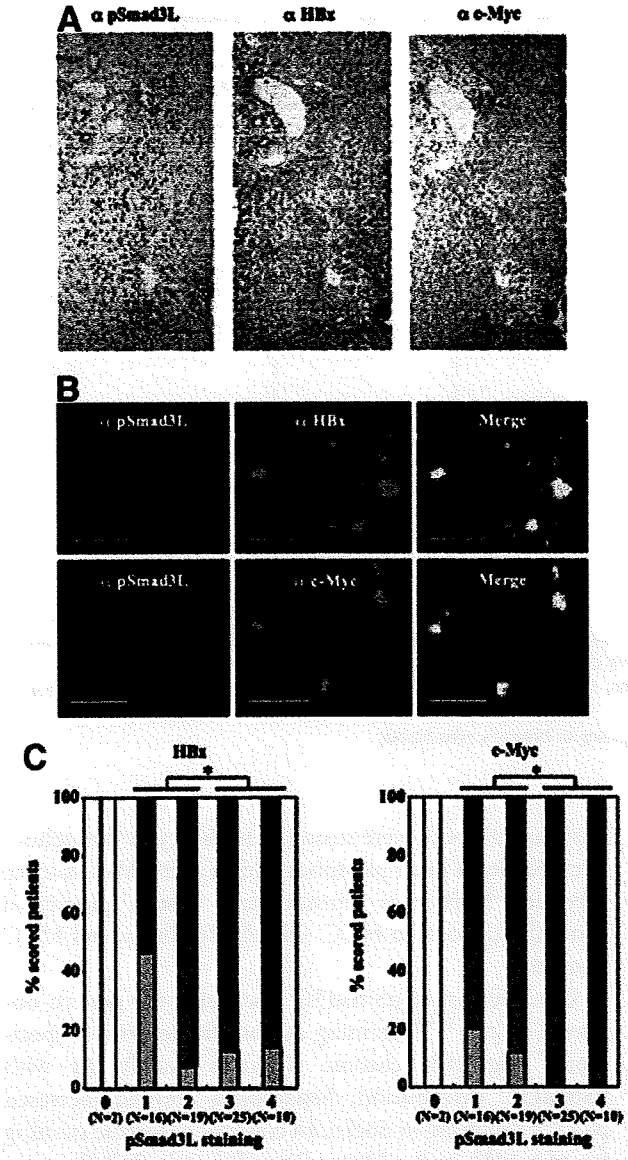

Fig. 3. HBx might be involved in c-Myc-mediated oncogenic activity in human chronic hepatitis B via the pSmad3L pathway. (A) Hepatocytes of chronic hepatitis B specimens from patient 3 in Table 2 showed diffuse immunostaining for pSmad3L, HBx, and c-Myc. All sections were counterstained with hemotoxylin (blue). Brown color indicates specific Ab reactivity. Bar = 50 μm. (B) pSmad3L in hepatocytic nuclei of chronic hepatitis B specimens was colocalized with HBx and c-Myc proteins. Sections of chronic hepatitis B tissues were stained for immunofluorescence to simultaneously detect pSmad3L (red) and HBx or c-Myc (green). Yellow color indicates overlap of proteins. Hepatocytes immunoreactive for pSmad3L showed colocalization of HBx (upper column) and c-Myc (lower column). Bar = 50 μm. (C) HBx and c-Myc expression increased in hepatocytes of chronic hepatitis B specimens as Smad3 was increasingly phosphorylated at the linker region. HBx and c-Myc expression was greater in hepatocytes with high phosphorylation at Smad3L (staining scored as 3 or 4) than in hepatocytes with staining scored as 0 to 2. The extent of HBx and c-Myc expression is indicated as that of pSmad3L positivity: □, 0; □, 1; ▩, 2; ■, 3; ■, 4. *$P < 0.05$.

regulation of pSmad3L was seen with progression of hepatic fibrosis and carcinogenesis. In cirrhotic liver and HCC, pSmad3L was far more abundant than in chronic hepatitis. In contrast, pSmad3C gradually decreased as disease stages progressed toward HCC (Fig. 4C, α pSmad3C panel).

We previously reported that Smad3L served as a substrate for JNK.[12] To address the functional relationship between activated JNK and Smad3L phosphorylation during hepatocarcinogenesis, we presently assayed kinase activity *in vitro*. Although JNK from normal liver showed little ability to phosphorylate Smad3 at the linker region, JNK from livers involved by chronic hepatitis B, cirrhosis, and HCC could directly phosphorylate Smad3L (Fig. 4D). These results suggested that JNK in preneoplastic liver tissues and HCC directly phosphorylated the linker region of Smad3.

Collectively, JNK/pSmad3L/c-Myc onogenic signaling in hepatocytes came to predominate while the tumor-suppressive pSmad3C/p21^{WAF1} pathway became quiescent as chronic hepatitis B progressed to cirrhosis and then HCC.

Selective Blockade of Linker Phosphorylation Abolishes pSmad3L-Mediated Cell Growth in HBx-Expressing Hepatocytes. pSmad3L, HBx, and c-Myc were colocalized in preneoplastic lesions including chronic hepatitis and cirrhosis (Fig. 3). These findings suggest that HBx oncoprotein might alter hepatocytic TGF-β signaling in chronic hepatitis B. We investigated this hypothesis using HBx-expressing hepatocytes. Selective blockade of linker phosphorylation by a mutant Smad3 lacking the JNK-dependent linker phosphorylation sites abolished pSmad3L-mediated cell growth in HBx-expressing hepatocytes (Supplementary Figs. 3-5). These results suggest that HBx activated the JNK/pSmad3L pathway, further promoting cell proliferation by up-regulating c-Myc transcription (Fig. 5).

Activation of the pSmad3L/c-Myc Pathway as HBx Transgenic Mouse Livers Progress Through Hyperplasia to HCC. We further investigated localization of pSmad3L, HBx, and c-Myc during HBx-induced hepatocarcinogenesis in HBx transgenic mouse livers. Beginning at the age of 2 months, HBx transgenic mouse liver showed centrilobular foci of cellular alteration with cytoplasmic vacuolation surrounding the central veins where bromodeoxyuridine was uptaken into the hepatocytes.[6]

In this hyperplastic mouse liver, phosphorylation at Smad3L was observed in hepatocytic nuclei in the centrilobular region, and distribution of pSmad3L was similar to those of HBx and c-Myc (Fig. 6A). pSmad3L, HBx,

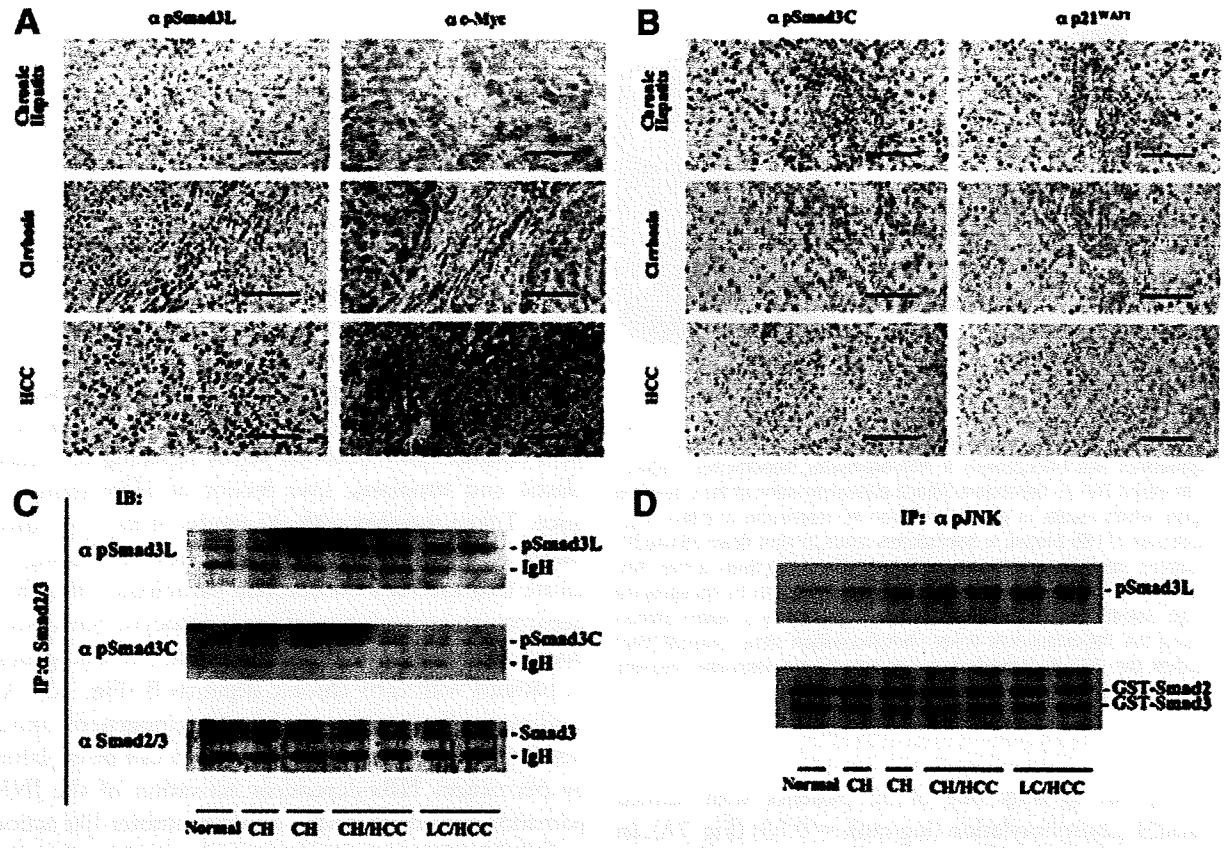

Fig. 4. As chronic hepatitis B progressed through cirrhosis to HCC, JNK/pSmad3L/c-Myc ongogenic signaling started to increase, whereas the tumor-suppressive pSmad3C/p21^{WAF1} pathway decreased. (A) pSmad3L and c-Myc increased as human chronic hepatitis B progressed through cirrhosis to HCC. (B) pSmad3C and p21^{WAF1} decreased as human chronic hepatitis B progressed through cirrhosis to HCC. All sections in A and B were counterstained with hemotoxylin (blue). Brown staining indicates specific Ab reactivity. Bar = 50 μm. (C) Immunoblotting of pSmad3L and pSmad3C in HBV-related chronic liver diseases. Cell lysates obtained from hepatocellular carcinoma (HCC) and surrounding nonneoplastic liver tissues including chronic hepatitis B (CH) or liver cirrhosis (LC) as well as uninvolved normal liver tissues from a patient with a metastatic liver tumor were subjected to anti-Smad3 immunoprecipitation (IP) and were then immunoblotted with each anti-pSmad3 Ab (upper panels). Relative amounts of endogenous Smad3 were determined via immunoblotting using anti-Smad3 Ab (bottom panel). (D) JNK in human HBV-related chronic liver tissue directly phosphorylated Smad3 at the linker region. Cell lysates obtained from HCC and surrounding nonneoplastic liver tissue including chronic hepatitis (CH) and liver cirrhosis (LC) from HBV-infected patients, as well as uninvolved normal liver tissue from a patient with a liver metastasis, were subjected to anti-phospho-JNK1/2 immunoprecipitation (IP), and were then mixed with bacterially expressed GST-Smad3 and GST-Smad2. After *in vitro* kinase assay, phosphorylation of Smad3L was analyzed via immunoblotting using anti-pSmad3L antibody (upper panel). Total Smad3 and Smad2 were determined via immunoblotting using anti-Smad2/3 Ab (lower panel).

and c-Myc were distributed diffusely in HCC specimens (Fig. 6B, HCC panel). Semiquantitative analyses of positivity for these molecules in HBx transgenic mouse livers also revealed that hepatocytic pSmad3L, HBx, and c-Myc increased as mouse liver progressed through hyperplasia to HCC (Fig. 6C). Double immunofluorescence studies in hyperplastic specimens confirmed that pSmad3L was colocalized in HBx- and c-Myc-immunoreactive hepatocytes (Fig. 6D).

Success in comparative study of HBx, pSmad3L, and c-Myc positivity during human and mouse hepatocarcinogenesis identified pSmad3L as a key regulatory element that offers a general framework for understanding the origins of HBV-related HCC.

Chronic Hepatitis B Patients with Hepatocytes Positive for pSmad3L and Negative for pSmad3C Increased Risk of HCC Development. We finally investigated whether phosphorylation levels of Smad3 could affect the risk of neoplastic evolution in the patients with chronic hepatitis B (Table 2). To compare HCC incidence, patients were classified into those with abundant (scores 3 to 4) and limited (scores 0 to 2) Smad3 phosphorylation in hepatocytic nuclei. HCC developed in six of 28 patients with abundant Smad3L phosphory-

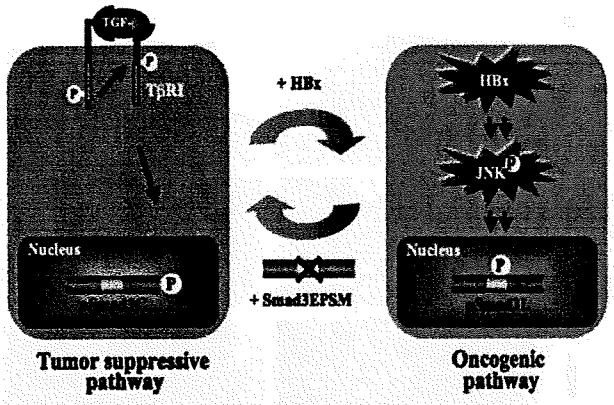

Fig. 5. Reversibility of Smad3-dependent signaling between tumor suppression and oncogenesis in HBx-expressing hepatocytes. Hepatocytes exhibit TGF-β–dependent Smad3 phosphorylation at the C-terminal region, which results in growth inhibition by repression of c-Myc. High expression of HBx protein in hepatocytes tends to shut down pSmad3C-mediated signaling and favor acquisition of constitutively active JNK-mediated pSmad3L signaling, which fosters cell growth by up-regulating c-Myc. Selective blockade of linker phosphorylation by a mutant Smad3 lacking the JNK-dependent linker phosphorylation sites (Smad3EPSM) restores the TGF-β–dependent tumor-suppressive response involving pSmad3C that is shown by parental hepatocytes.

lation, but in only one of 32 patients with limited Smad3L phosphorylation (log-rank = 0.03) (Fig. 7A). In contrast, HCC developed only in the patients with limited Smad3C phosphorylation, and no patients with abundant hepatocytic pSmad3C developed HCC (log-rank = 0.009) (Fig. 7B).

Several studies have analyzed risk factors for HCC occurrence in patients with HBV-related chronic liver disease, including elevated plasma HBV DNA[24] and seropositivity for hepatitis B e antigen.[26] In the univariate analysis, HCC occurrence in high pSmad3L positivity ($P = 0.01$), low pSmad3C positivity ($P = 0.03$), and plasma HBV-DNA levels of more than 5.0 log copies/mL ($P = 0.05$) showed P values less than 0.10, thus being significantly associated with HCC (Table 5). All variables with statistical significance in the univariate analysis were entered in the multivariate analysis, and high pSmad3L and low pSmad3C positivity were considered significantly predictive of HCC development within 12 years. Hepatocytic positivitiy for pSmad3L and pSmad3C should allow us to distinguish chronic hepatitis B patients at high and low risk for the development of HCC in near future.

Discussion

In patients with chronic hepatitis B, persistent HBV infection is clearly the primary inducer of HCC.[1-7] Comparative studies that seek to identify conserved oncogenic signaling common to HCC in both humans and experimental animals will help to eventually identify the molecular pathways that drive the development of HCC.[27] Much is known about the morphologic changes of cells and tissues that precede and accompany development of HCC in humans, allowing earlier diagnosis in some instances.[28] A variety of molecular alterations have been detected in fully developed HCC and to a lesser extent in morphologically defined preneoplastic precursor lesions.[29] Our current studies compared pSmad3L- and pSmad3C-mediated signaling in biopsy specimens of chronic hepatitis, cirrhosis, or HCC from 90 patients with chronic HBV infection versus signaling in preneoplastic and neoplastic liver lesions of HBx transgenic mice. Taken together with the results of *in vitro* experiments using HBx-expressing hepatocytes, our findings indicate that the HBx oncoprotein participates directly in hepatocarcinogenesis by shifting hepatocytic Smad3-mediated signaling from tumor suppression to oncogenesis in patients with early chronic hepatitis B (Fig. 7C). According to the two-step model of carcinogenesis (initiation and promotion), tumor formation can be explained by permanent HBx-dependent activation of the JNK/pSmad3L cascade that has a tumor promoter-like action.

HCC is a human neoplasm associated with viral infection.[1,3] At present, hepatitis virus–associated carcinogenesis can be seen as a multifactorial process that includes both direct and indirect mechanisms.[19] A major factor in the process of HCC development is the host immune system.[30] Chronic inflammation, degeneration, and regeneration induced by the host cellular immune response are common to a variety of human liver diseases, and subsequent cellular proliferation might increase the risk of cancer. We previously reported that increased phosphorylation of Smad3L and decreased phosphorylation of Smad3C were associated with an increased risk of HCV-related HCC.[20] Similarly to HCV-related chronic liver disease, strong pSmad3L positivity was observed in the late stages of HBV-related chronic liver disease (F3 to F4) (Fig. 1C). Considering the development of HCC in HCV core gene-transgenic mice,[31] hepatitis viruses themselves together with the host immune response might promote human hepatocarcinogenesis via the JNK/pSmad3L pathway during the late stage of the carcinogenic process in both HBV- and HCV- related chronic liver disease.

However, HBV and HCV have different roles in human hepatocarcinogenesis when early chronic hepatitis (F1 to F2) is considered. The histological severity of-HCV-related liver disease correlates closely with the risk

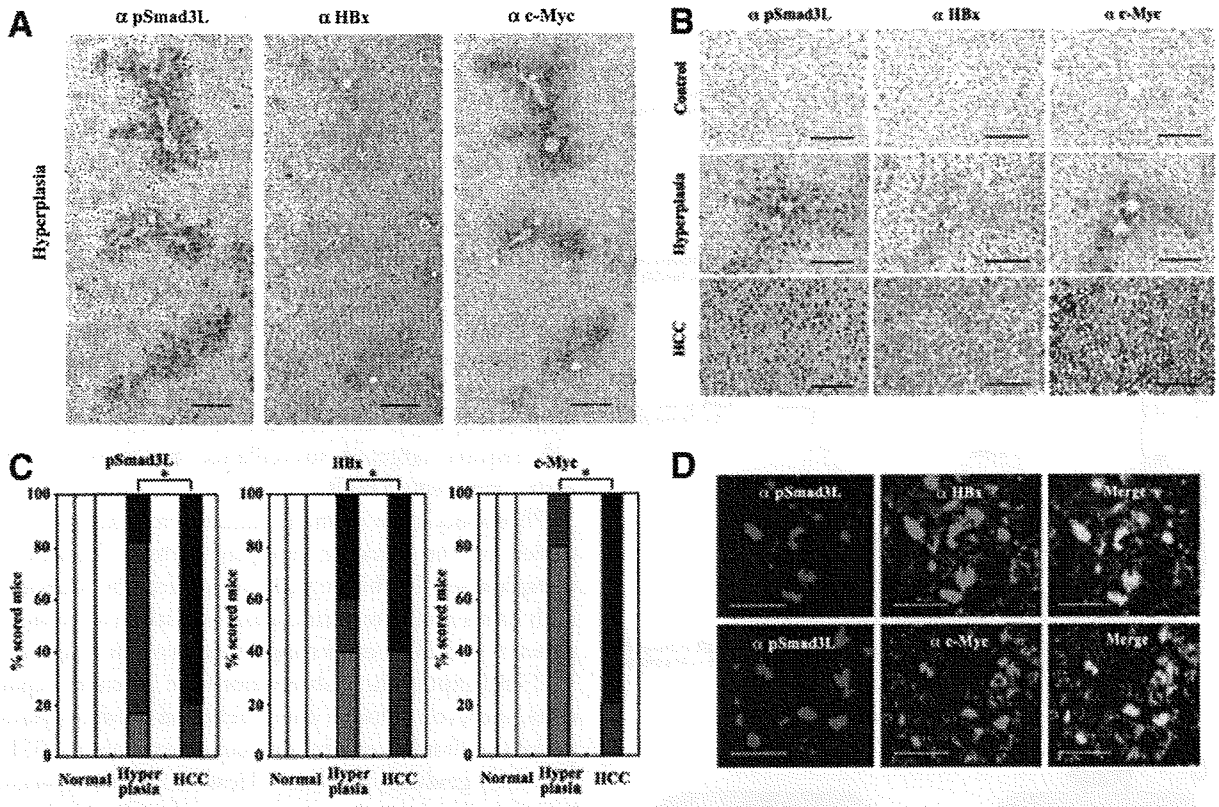

Fig. 6. The pSmad3L/c-Myc pathway was activated as HBx transgenic mouse liver progressed through hyperplasia to HCC. (A) Distribution of pSmad3L, HBx, and c-Myc in hyperplastic specimens from HBx transgenic mouse liver. (B) Distributions of pSmad3L, HBx, and c-Myc in normal liver, hyperplasia, and HCC specimens from HBx transgenic mice. Immunostaining for pSmad3L, HBx, and c-Myc was present in hyperplastic hepatocytes surrounding central veins in HBx transgenic mouse liver [(A) and (B), hyperplasia panels], and was distributed diffusely in HCC specimens [(B), HCC panel]. All sections were counterstained with hemotoxylin (blue). Brown color indicates specific Ab reactivity. Bar = 50 μm. (C) Hepatocytic pSmad3L, HBx, and c-Myc increased as HBx transgenic mouse liver progressed from hyperplasia to HCC. Staining for pSmad3L, HBx, and c-Myc was detected minimally in normal mouse livers, but was strongly up-regulated in neoplastic livers. In HCC, pSmad3L, HBx, and c-Myc were significantly greater than in livers with hyperplasia. $^*P < 0.05$. Extent of pSmad3L, HBx, and c-Myc: □, 0; ▨, 1; ▩, 2; ■, 3; ■, 4. (D) Hepatocytic pSmad3L in hyperplastic specimens from HBx transgenic mouse liver was colocalized with HBx and c-Myc. Hyperplasia sections of HBx transgenic mouse livers were stained for immunofluorescence to simultaneously detect pSmad3L (red) and HBx or c-Myc (green). Yellow color indicates overlap of proteins. Hepatocytes immunoreactive for pSmad3L showed colocalization of HBx (upper column) and c-Myc (lower column). Bar = 50 μm.

of HCC.[32] In contrast, HCC occasionally develops in healthy HBV surface antigen carriers, who are persistently infected with HBV but have normal liver function parameters and no necroinflammation.[33] This indicates that HBV itself has a direct influence on hepatocarcinogenesis in early chronic hepatitis B. Although integration of the viral genome into chromosomal DNA has not been reported in patients with HCV infection, integration of HBV has been detected in almost all cases of chronic hepatitis B,[3] leading to activation of the HBx-mediated oncogenic pathway.[4] It is noteworthy that HCC developed in patient 10 (Table 2), who showed strong pSmad3L positivity of hepatocytic nuclei but had minimal necroinflammatory activity (A1) or fibrosis (F1). In summary, HCV contributes indirectly to the development of HCC through chronic inflammation in early chronic hepatitis C. In contrast, HBV directly triggers the JNK/pSmad3L oncogenic pathway in early chronic hepatitis B, thus playing a role beyond mere stimulation of the host immune response.

Our findings also open up a new avenue to understanding the development and progression of hepatic fibrogenesis.[34] Whereas HSCs have traditionally been considered as the principal source of liver fibrosis, mature hepatocytes can acquire a mesencymal phenotype and perform the functions of activated HSC—that is, they can contribute to fibrogenesis.[35,36] In support of this notion, pSmad3L-mediated signaling promotes liver fibrosis by hepatocytes as well as activated HSCs during long-standing carcinogenesis.[13,18,20] In this manner, either HBV- or HCV-related chronic hepatitis progresses through fibrogenesis to HCC.